5-2013

Post-Market Surveillance of Total Knee Replacement Combining Clinical Outcomes and Quantitative Image Processing Techniques

Leah Nunez
Clemson University, trevnun9@aol.com

POST-MARKET SURVEILLANCE OF TOTAL KNEE REPLACEMENT COMBINING CLINICAL OUTCOMES AND QUANTITATIVE IMAGE PROCESSING TECHNIQUES

A Dissertation
Presented to
the Graduate School of
Clemson University

In Partial Fulfillment
of the Requirements for the Degree
Master of Science
Bioengineering

---

by
Leah Nunez
May 2013

Accepted by:
Melinda Harman, PhD; Committee Chair
David Kwartowitz, PhD
Thomas Pace, MD

Abstract

Total knee replacement (TKR) is a successful procedure for the relief of pain, correction of deformity, and restoration of function in patients with knee arthritis.[1-3] In the United States, the number of primary TKR surgeries performed in 2030 is projected to be between 2,938,000 to 4,136,000 and revision surgeries between 193,000 to 381,000.[4] Osteolysis, pain, and aseptic loosening are the most common causes of revision TKR surgery.[5] The purpose of this thesis is to complete assessments for post-market surveillance of total knee replacement (TKR) targeting areas for improving polymer bearings through evaluation of clinical outcomes and analysis of prosthesis retrieved after in vivo function. The overall objective of this thesis is to use such assessments for comparing different polyethylene types (conventional and highly cross-linked) and articular designs (cruciate retaining and posterior stabilized) currently in use for TKR. This overall objective is accomplished in three specific aims.

The first aim completes a retrospective clinical outcome study of 9 patients (10 cases), fully describing pre-operative and intra-operative surgical decision models for the clinical evaluation and surgical treatment of TKR patients with focal areas of periprosthetic osteolysis. Patients have not exhibited any further complications associated with osteolysis after 5.1±2.4 years of follow up. Routine radiographic exams show total incorporation of the graft material into the previously lytic regions in all patients.

The second aim acquires polyethylene inserts that have functioned in patients and develops a custom analysis program with a graphical user interface (GUI) for completing

quantitative assessments of damage patterns observed on the polyethylene inserts' surfaces. The developed analysis software outputs accurate and reproducible results comparable to ImageJ software. Additionally, the developed GUIs allow for user friendly image digitization, processing and analysis and eliminate of the need for users to have extensive computer programming knowledge.

The third aim uses the image-based measurement tool developed in the second aim to assess damage patterns occurring on the retrieved polyethylene tibial inserts with different types of polyethylene, namely conventional and highly cross-linked ultrahigh molecular weight polyethylene, and on tibial inserts with different types of articular constraint, namely posterior cruciate ligament retaining and posterior stabilized. The results of this aim provide unique insight into the effects of the physiological environment in which the TKR devices performed that simulations have not yet been able to replicate and provide data on the effects of changes to TKR design, including polyethylene types and articular constraints.

Dedication

I dedicate this thesis to my parents, who supported me each step of the way. Without their constant and unwavering support, I would not be where I am today.

Acknowledgements:

The authors acknowledge Sandra Fowler and Becky Snider for their assistance with the medical record reviews used in Aim 1. Dr. David Kwartowitz and Lucas Schmidt are acknowledged for their assistance in the development of the GUI. CU-REPRO is acknowledged for its role in implant procurement. The authors would like to acknowledge Clemson University Department of Bioengineering Start Up Fund for Dr. Melinda Harman for funding.

Table of Contents

Abstract ……...ii

Dedication……...iv

Acknowledgements ……v

Chapter 1 An Introduction 1

Purpose and Aims: 6

Aim 1. Characterization of Surgical Options for Treatment of Osteolysis after Total Knee Replacement 9

Aim 2. Acquire Retrieved Polyethylene Inserts and Create an Image-based Measurement Tool with Graphical User Interface for Measuring Damage Modes 9

Aim 3. Distinguish Variations in Damage Distribution Comparing TKR Designs with Different Types of Polyethylene and Different Articular Constraint 10

Chapter 2 Characterization of Surgical Options for Treatment of Osteolysis after Total Knee Replacement 11

Introduction 11

Materials and Methods 13

Results 16

Chapter 3 Acquire Retrieved Polyethylene Inserts and Create an Image-Based Measurement Tool with Graphical User Interface for Measuring Damage Modes 24

Introduction 24

Materials and Methods 27

Results 33

Discussion 35

Chapter 4 Distinguish Variations in Damage Distribution Comparing TKR Designs with Different Types of Polyethylene and Different Articular Constraint 43

Introduction 43

Materials and Methods 54

Results 57

Discussion 65

Table of Contents (Continued)

Chapter 5 Conclusions and Recommendations..... 74
References:..... 79

List of Figures

Figure 1. Posterior stabilized TKR.. 6
Figure 2.Posterior stabilization cam-post engagement 7
Figure 3. PCL retaining TKR..... 8
Figure 4. Pre-operative surgical decision model..... 21
Figure 5. Intra-operative surgical decision model. 22
Figure 6. Radiographs of a 67 year old male who underwent bone grafting and isolated insert exchange for femoral osteolytic region..... 22
Figure 7. Radiographs for a 64 year old female patient who underwent bone grafting and isolated insert exchange. 23
Figure 8. Damage Mode Atlas images acquired through the microscope. 36
Figure 9. Damage Mode Atlas images acquired through the microscope. 37
Figure 10. Descriptions of distinct features characteristic for each damage mode 38
Figure 11. Five distinguishing features for each damage mode 39
Figure 12. Image contouring GUI process..... 40
Figure 13. Display GUI process..... 41
Figure 14. Image Standards.. 42

List of Tables

Table 1. Image J and MatLab GUI Accuracy Validation Data 34
Table 2. ImageJ and MatLab GUI Reproducibility Validation Data 34
Table 3. Patient Demographics for Comparison Groups 56
Table 4. Compare UHMWPE 1 Results Summary 59
Table 5. Compare UHMWPE 2 Results Summary 59
Table 6. Compare CONSTRAINT 1 Results Summary 60
Table 7. Compare CONSTRAINT 2 Results Summary 60
Table 8. Compare CONSTRAINT 3 Results Summary 61
Table 9. Compare UHMWPE 1 Frequency and Area Affected Percentages 62
Table 10. Compare UHMWPE 2 Frequency and Area Affected Percentages 63

Chapter 1
An Introduction

Total knee replacement (TKR) is a successful procedure for the relief of pain, correction of deformity, and restoration of function in patients with knee arthritis.[1-3] Between its inception in 1999 and December 31st, 2007, the New Zealand Joint Registry has obtained data on 34,458 primary TKRs.[5] In the United States, the number of primary TKR surgeries performed in 2030 is projected to be between 2938000 to 4136000 and revision surgeries between 193000 to 381000.[4]

Many registries, including both the New Zealand Joint Registry, use the Oxford hip and knee outcome questionnaires to assess the outcome after primary total hip and knee replacement surgeries.[5,6] Other outcome measures include the Harris and Charnley hip scores, the Hospital for Special Surgery knee scores, and the Knee Society Score.[6,7] In the United States, the KSS is the primary method used to score patients after TKR and it assess pain, stability, and range of motion with deductions for flexion contracture, extension lag, and misalignment.[7]

Some of the known complications after TKR include polyethylene wear and osteolysis, which is most commonly the result of the production of biologically active polyethylene debris.[8] Osteolysis, pain, and aseptic loosening are the most common causes of revision TKR surgery.[5] A little over 50% of revision TKR surgeries are caused by polyethylene wear, presenting as either isolated radiological findings or symptomatic wear-debris synovitis with eventual osteolysis compromising prosthetic fixation.[9] Of that approximate 50% of revision cases, nearly two-thirds are due to osteolysis, with the

chance of revision surgery increasing about 0.20% each year of follow-up for the first 27 years.[9]

One of the issues associated with polyethylene wear is the migration of the debris particles into nearby bone tissue. The polyethylene particles induce a foreign body response, ultimately resulting in frustrated phagocytosis that induces regions of necrosis in the bone tissue and osteolysis. The body's reaction to a foreign material begins with inflammation. The progression of inflammation and the foreign body cellular response requires the migration of monocytes from the blood stream to the location of the debris. Once the macrophages have arrived at the location, they begin to attempt to remove the foreign body through phagocytosis. The polyethylene debris typically generated in can range in size, from 0.58 μm to 5.23 μm.[10] In the event that a single macrophage cannot ingest a debris particle, it can fuse with adjacent macrophages to form foreign-body giant cells. The exact mechanism that leads to the fusion has not yet been determined but may be receptor mediated.[11] It is known that IL-4 induced molecules must be present on both cells in order for the fusion to occur.[11] When macrophages and foreign-body giant cells adhere to the surface of a biomaterial, they create a unique microenvironment between their cell membranes and the surface. In frustrated phagocytosis the macrophages and foreign-body giant cells release mediators of degradation such as reactive oxygen intermediates, degradative enzymes, and acid into their created microenvironment and results in the release of inflammatory mediators that stimulate bone resorption.[11]

Polyethylene wear can be generated on both the bearing and backside surfaces of the tibial insert, with the predominate source of polyethylene debris generation believed

to be the articulation of the femoral component on the bearing surface of the insert.[12-14] Wear on the backside surface of the insert is believed to be an additional source of polyethylene debris contributing to tibial metaphyseal osteolysis.[12] Holes in the tibial baseplate, tibial fixation screws, and areas of discontinuous porous coating or cement interface are possible conduits for the debris into the bone tissue.[8] Periprosthetic osteolysis is mainly caused by small particulate debris stimulating a foreign-body cellular response that results in bone resorption.[8]

There are sixteen main damage modes observed in retrieved polyethylene tibial inserts which can be readily observed at low magnification, such as in optical microscopy.[15] In order to ensure correct identification, use of a pictographic damage atlas is important as identification of damage modes based on descriptions obtained from literature can be inconsistent. In "A pictographic atlas for classifying damage modes on polyethylene," an illustrated reference guide of damage modes (Damage Mode Atlas) for damage observed on polyethylene was developed and a training protocol for new researchers validated.[15] Use of the Damage Mode Atlas was able to increase the rate of correct identification of damage modes and improved inter-rater reliability.

There are two types of design for TKRs that are used to control joint stability – posterior stabilized or posterior cruciate ligament (PCL) retaining. Depending upon the patient's needs, a surgeon can choose either design. Fig. 1 displays the articulation of a posterior stabilized design. Image B in Fig. 1allows for visualization of the cam-box articulation. Fig. 3 displays the articulation of a PCL retaining design. Overall, PCL retaining and posterior stabilized TKR designs have similar clinical outcomes.

Use of posterior stabilized TKRs can be dependent upon surgeon preference, availability, or the condition of the surrounding soft tissues and posterior cruciate ligament (PCL). The PCL is the strongest of the four ligaments in the knee, providing it with stability while pulling back the femur posteriorly onto the tibia during "roll-back", thereby preventing posterior translation of the tibia.[16] The removal of the PCL thus necessitates the addition of a post to the polyethylene insert that articulates with the metal cam portion of the femoral component in order to restore stability to the joint as demonstrated in Fig. 1. The cam-post mechanism was developed to induce posterior femoral translation during deep knee flexion with the goal of increasing maximum knee flexion; different designs allow for different degrees of flexion, ranging from between 20° to 65° of flexion.[17,18] One of the problems associated with TKR that posterior stabilized knees sought to overcome was that patients rarely flex the knees beyond 120° after surgery.[19] Posterior stabilized TKRs have been evaluated in terms of patient function, knee kinematics, rotational kinematics, risk of post fracture, survivorship, rates of osteolysis, range of motion, and clinical results.

In some cases, the PCL can be retained in patients and a PCL retaining TKR design is utilized. There has been some debate about whether the PCL should remain intact or be resected during the TKR procedure, with soft tissue conditions and surgeon preference playing a role in the decision making process. Some potential disadvantages associated with this design are PCL rupture, patellofemoral malalignment, and posteromedial polyethylene wear and may influence survivorship of the prosthesis.[20] Overall, PCL retaining fixed-bearing TKR designs are highly successful with the need for

additional surgery occurring at approximately 0.4% per year for the first 27 years[9] and survivorship rates after 10 years at 87% to 95.7%.[20] Evaluations of PCL retaining TKR designs include analysis of long-term survival, tibial translation, maximum flexion, and anteroposterior stability.

Both standard and highly cross-linked UHMWPE are used in total knee replacements. Since the creation of the total knee replacement, multiple modifications have been completed in an attempt to improve the functionality and life cycle of the device. Osteolysis has been associated with backside wear and tibial modularity, the polyethylene sterilization method and stock, and the design of the posterior stabilized tibial post.[21] Other factors that contribute to polyethylene debris generation and osteolysis include patient age, patient activity level, and surgical factors. Cross-linked ultra-high molecular weight polyethylene (UHMWPE) was developed to reduce volumetric wear in both hip and knee prostheses in comparison to standard UHMWPE.[22]

Traditionally, UHMWPE is cross-linked through gamma or electron-beam radiation of a ram-extruded bar stock or compression-molded sheet polyethylene at a dose greater than 4 MRads.[23] Thermal treatment eliminates or reduces free radicals while enhancing the saturation of crosslinking. Implants can then be machined from the treated UHMWPE. If a manufacturer prefers remelting, they will typically sterilize the insert using ethylene oxide gas or gas plasma techniques; if annealing is preferred, then conventional gamma sterilization in an inert environment is used for sterilization.[23]

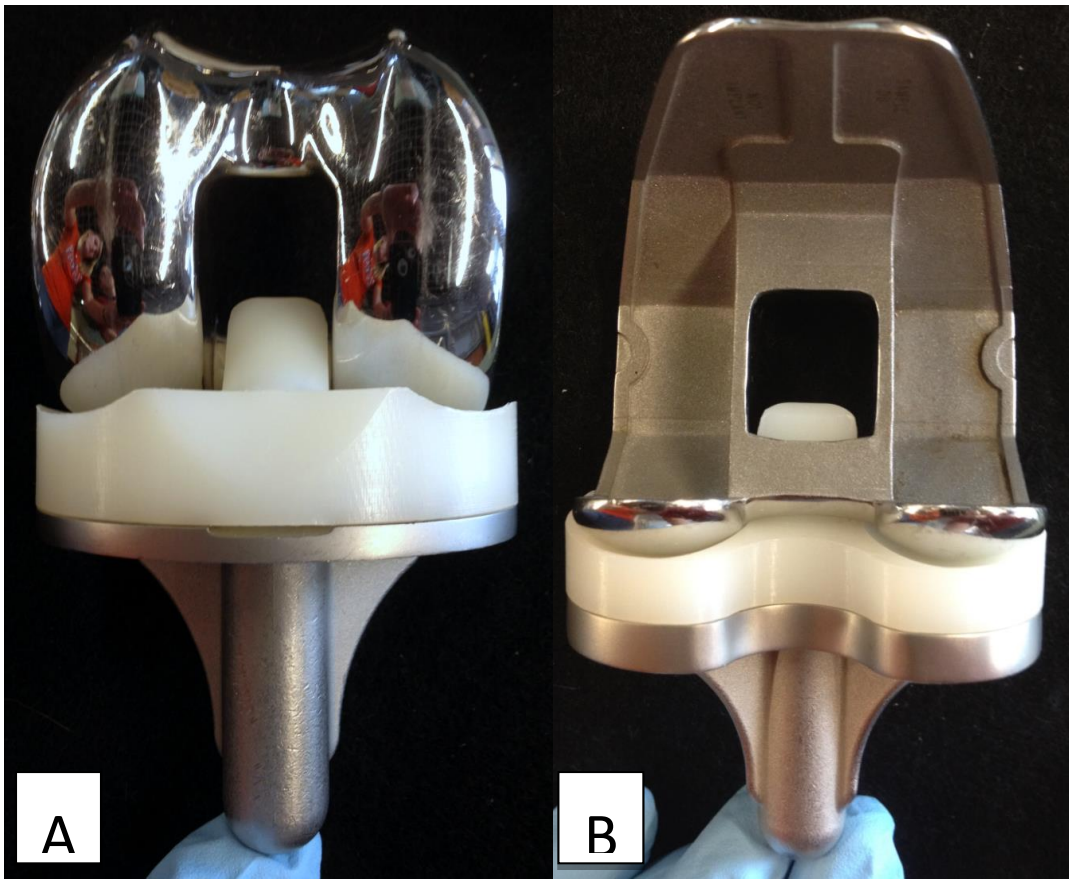

Figure 1. Posterior stabilized TKR. (A) Anterior view of an articulating femoral component on the posteriorly stabilized UHMWPE tibial insert with the post easily visualized. (B) Posterior view of the articulating femoral component.

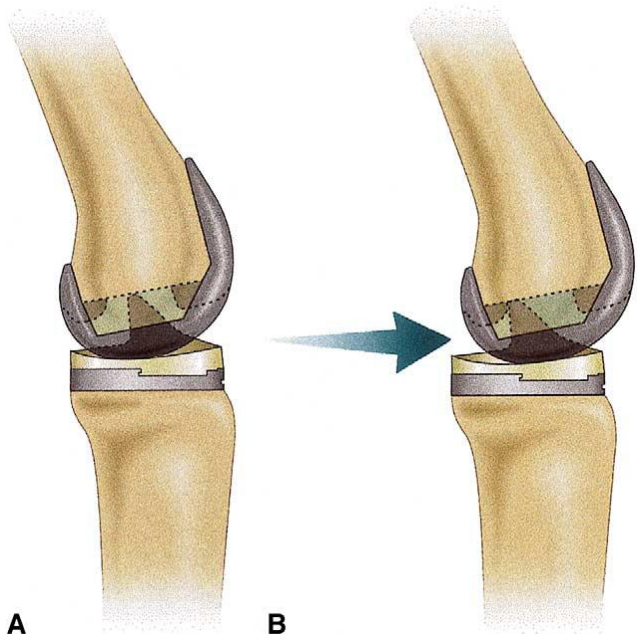

Figure 2. (A) At the time of load application, the posterior stabilized prosthesis does not have a cam and post engagement. (B) Forward motion of the femoral component can occur until the cam and post engage. Different designs allow for different amounts of forward sliding of the femur.[17]

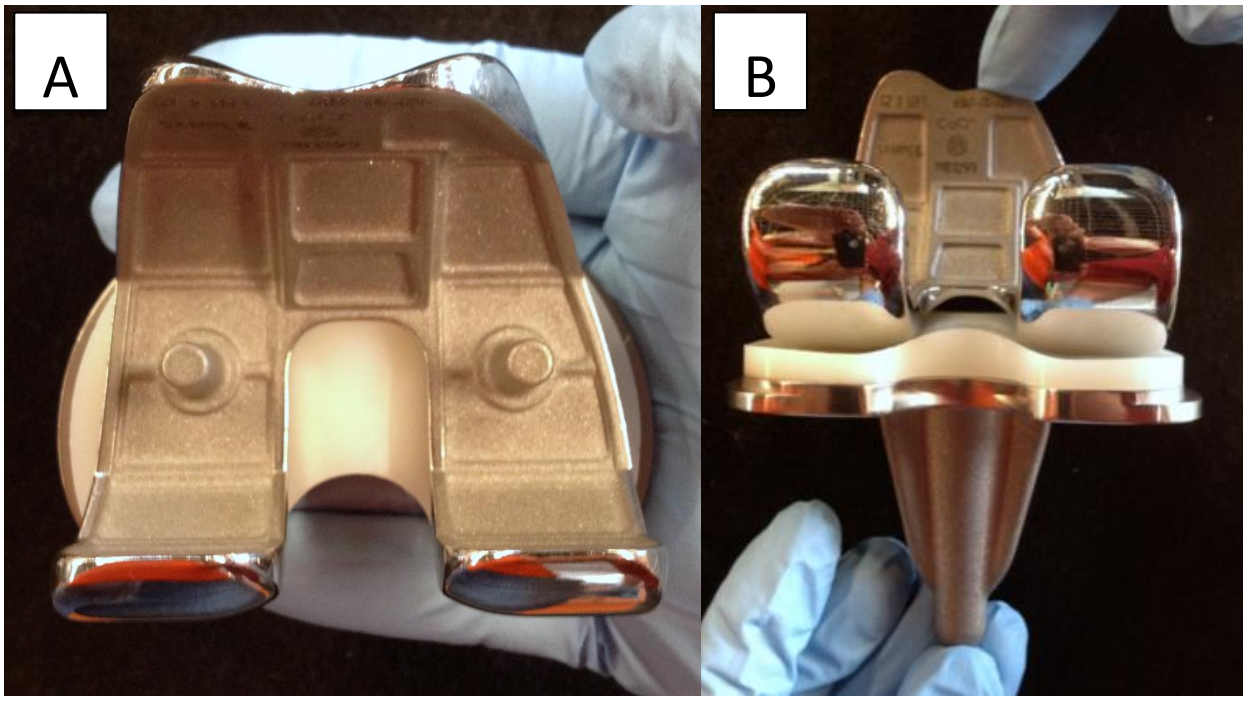

Figure 3. PCL retaining TKR. (A) View allowing visualization of design that allows for retention of PCL. (B) Posterior view of device with space between the condyles for ligament retention.

Purpose and Aims:

The purpose of this thesis is to complete assessments for post-market surveillance of total knee replacement (TKR) targeting areas for improving polymer bearings through evaluation of clinical outcomes and analysis of prosthesis retrieved after in vivo function. The overall objective of this thesis is to use such assessments for comparing different polyethylene types (conventional and highly cross-linked) and articular designs (cruciate retaining and posterior stabilized) currently in use for TKR. This overall objective is accomplished in three specific aims.

Aim 1. Characterization of Surgical Options for Treatment of Osteolysis after Total Knee Replacement

Osteolysis, pain, polyethylene wear, and aseptic loosening are all indications for revision surgery. The standard surgical treatment is removal and replacement of the TKR, potentially with augmentation such as long intramedullary stems. Other surgical options include isolated insert exchange and insert exchange and bone grafting to fill osteolytic defects. The objective of Aim 1 is to complete a retrospective clinical outcome study, fully describing pre-operative and intra-operative surgical decision models for the clinical evaluation and surgical treatment of TKR patients with focal areas of periprosthetic osteolysis. It is hypothesized that for such TKR patients, decision models involving insert exchange and use of a novel surgical technique can be a viable alternative to complete TKR revision.

Aim 2. Acquire Retrieved Polyethylene Inserts and Create an Image-based Measurement Tool with Graphical User Interface for Measuring Damage Modes

The objective of Aim 2 is to acquire polyethylene inserts that have function in patients and develop a custom analysis program with a graphical user interface (GUI) for completing quantitative assessments of damage patterns observed on the polyethylene inserts' surfaces. It is hypothesized that the GUI interface will provide seamless transfer between user controlled functions of image selection, calibration, digitization, damage mode identification, damage area and location measurement, damage pattern display, and

data output. In this manner, consistent and accurate assessments of damage patterns of retrieved tibial inserts can be accomplished by users without advanced training in software programming. Through Clemson University's implant retrieval program, Retrieval of Explants Program and Registry in Orthopaedics (REPRO), fifty tibial inserts were obtained and assessed using the image-based measurement tool developed in this aim.

Aim 3. Distinguish Variations in Damage Distribution Comparing TKR Designs with Different Types of Polyethylene and Different Articular Constraint

The objective of Aim 3 is to use the image-based measurement tool developed in Aim 2 to assess damage patterns occurring on the retrieved polyethylene tibial inserts with different types of polyethylene, namely conventional and highly cross-linked ultrahigh molecular weight polyethylene (UHMWPE), and on tibial inserts with different types of articular constraint, namely cruciate-retaining and posterior-stabilized. It is hypothesized that tibial inserts fabricated from highly cross-linked UHMWPE will have damage modes occurring at different frequencies compared to the conventional UHMWPE inserts. It also is hypothesized that tibial inserts with the posterior stabilized constraint will have damage patterns located more posterior than the inserts with PCL retaining constraint.

Chapter 2
Characterization of Surgical Options for Treatment of Osteolysis after Total Knee Replacement

Introduction

Periprosthetic osteolysis is a known complication after cementless total knee replacement (TKR), including cases in which the implant is well fixed and properly aligned.[24-32] A viable treatment option for progressive periprosthetic osteolysis observed after total hip replacement (THR) is polyethylene liner exchange and bone grafting of the osteolytic lesions.[33] Using this treatment method as a model, a polyethylene insert exchange and bone grafting technique was developed to treat patients with progressive periprosthetic osteolysis in cementless TKR. Due to the decrease in survivorship associated with complete TKR revision,[34] combined with the increasingly younger patients undergoing TKR, this method may be a viable option for a select group of TKR patients with osteolysis.

Of the approximate 50% of revision cases caused by polyethylene wear, nearly two-thirds are due to osteolysis.[9] Typical movements that generate polyethylene wear on the articular surface include rolling, sliding, and rotational motions. These movements may lead to delamination, pitting, and fatigue failure of the bearing surface.[8] Backside wear is another source of polyethylene particular debris generation and is generated by micromotion between the insert and the metal tibial component as a result of loosening of the locking mechanism. Polyethylene debris has been shown to stimulate bone resorption, synovitis, granuloma formation, and implant loosening.[11,28]

Osteolysis is a well-recognized complication after THR that presents diagnostic and treatment challenges.[33]Among patients showing polyethylene wear and acetabular osteolysis who are otherwise asymptomatic for pain without visible cup loosening or malalignment, treatment options include isolated liner exchange or revision of the liner and cup, both in combination with retroacetabular bone grafting.[35] The conditions that qualify a patient for isolated liner exchange are controversial, and as a result, there is debate over the use of this treatment method.[33,36] Studies have shown that isolated liner exchange has neutral to favorable outcomes when compared to revision THR of the liner and cup, with infrequent minor complications and an absence of osteolysis progression.[33,35,36]

Similar to THR, periprosthetic osteolysis associated with polyethylene wear can occur adjacent to the metal components of TKR. The traditional course of treatment is complete TKR revision,[26] but bone grafting and isolated insert exchange may be an option for some osteolytic patients, given the lessons learned from THR. However, isolated insert exchange after TKR has had variable success, suggesting that clear indications and surgical decision models are needed. Rerevision rates of 16% to 25% have been reported at less than five year follow up after isolated insert exchange for instability, wear, and osteolysis in TKR.[37,38] In contrast, excellent results have been reported for treating focal osteolysis with bone grafting and isolated insert exchange, with rerevision necessary in less than 5% of cases and no evidence of component loosening.[39]

The purpose of this study is to systematically assess patients who presented with progressive periprosthetic osteolysis adjacent to well-fixed and well-aligned uncemented

TKR and were treated with bone grafting and isolated insert exchange. We define the pre-operative and intra-operative surgical decision models used in the clinical evaluation and surgical treatment of these patients and present a retrospective review of outcomes at 1 to 10 years follow up.

Materials and Methods

A retrospective review was completed for 9 patients (10 cases) who presented with osteolysis adjacent to well-fixed and well-aligned uncemented TKR and were treated with bone grafting and isolated exchange of the tibial polyethylene insert and retention of the femoral and tibial components. The senior surgeon (Thomas Pace) performed all index TKR surgeries between December 1996 and January 2003 and all subsequent bone grafting and isolated insert exchanges between December 2002 and December 2011. Approval for clinical records review was obtained from Greenville Hospital System's Institutional Review Board.

At index TKR, all patients presented with an underlying diagnosis of osteoarthritis. Surgical technique included a subvastus approach with resection of the posterior cruciate ligament, a tibial cut aligned parallel with the posterior slope of the articular surface, and the patella left unresurfaced. All knees were implanted with an uncemented TKR prosthesis (Natural Knee II with Ultracongruent insert, Sulzer Medica, Austin, TX). Femoral and tibial component fixation was enhanced by spreading the cut bone surfaces with a bone slurry reamed from the cancellous bone of the tibial wafer,[40,41]

with five tibial baseplates further augmented with insertion of cancellous screws. All patients were followed during routine annual clinical evaluations, including radiographic and physical exams. Knee Society Scores preceding bone grafting and isolated insert exchange for these patients averaged 96.4 ± 5.3.

The main indication for subsequent surgery, including bone grafting and isolated insert exchange, was periprosthetic osteolysis observed on routine clinical radiographs. All patients were counseled for possible complete revision of all components and the risks associated with the insert exchange and bone grafting procedure were discussed in depth. The pre-operative surgical decision for bone grafting and isolated insert exchange, rather than complete revision, was indicated in patients presenting with osteolysis with well-aligned components that appeared well-fixed on pre-operative clinical radiographs (Fig. 4). If the osteolytic defect is significant enough to potentially threaten mechanical stability, or a small lesion that increases in size in a six month to a year of follow-up, then the window procedure should be considered as a treatment option. If the lesion disrupts the cortical bone, then the window procedure should not be considered as a treatment option. The maximum lesion size that was operated on in this study was 5.5cm x 6.0cm, which was defined as a large lesion. The intra-operative surgical decision to proceed with bone grafting and isolated insert exchange was indicated after the surgeon manually confirmed the joint stability and fixation of all components and confirmed localization of the osteolytic regions (Fig. 5). At the time of reoperation, the surgical instruments necessary for a complete revision were available in the event that the metal components were not firmly fixed.

The surgical technique for bone grafting and isolated insert exchange followed a uniform intra-operative surgical decision model (Fig. 5). Upon opening the joint, stability and fixation of the femoral and tibial components were manually verified by attempting to remove the femoral and tibial components with the extraction instruments. The polyethylene tibial inserts were removed and visually inspected, noting no gross evidence of delamination on the articular surfaces and scratches and deformation into recessed features on the backside surface. Surgical instruments were used to probe along the bone interface of the femoral component to detect any osteolytic regions. If the regions were discovered, then the cystic area was curetted and bone graft materials were used to fill the defect. The tibial cystic area was then addressed by making a 1cm by 1cm window medial to the tibial anterior crest, curettage of the tibial osteolytic lesion and subsequently packing the defect with bone graft material. The window was then replaced on the proximal tibia and secured with sutures in the overlying soft tissues. A new non-ultracongruent polyethylene insert (Sulzer Medica) was snapped onto the existing tibial baseplate, with selection of a less congruent bearing surface in all but the first case. All knees retained their initial PE insert size and thickness, except one knee presenting with excessive pre-operative tightness in which the insert was downsized from 11mm thickness to 9 mm thickness to allow for better motion. The bone graft material utilized included cancellous allograft, demineralized bone matrix putty, or a combination of the two. The decision for which material to use was dependent on availability at time of surgery.

At last follow-up, clinical outcomes were assessed according to Knee Society

guidelines [7] and radiographs taken before and after the bone grafting and isolated insert exchange procedure were reviewed (Fig. 6 and Fig. 7). On pre-revision films frontal and sagittal plane radiographs, radiolucent lines were assessed and osteolytic lesions were classified according to their largest dimension measured on the radiographs. Osteolytic lesions were classified as small if the dimension was less than 2 cm, medium if between 2 cm to 4 cm, and large if greater than 4 cm. On post-operative films, radiolucent lines and the extent of defect healing and graft incorporation were assessed by a fellowship trained arthroplasty surgeon not involved with the index or revision surgery (Brandon Broome).

Results

There were seven male patients and two female patients treated with bone grafting and isolated insert exchange, including one patient with bilateral procedures completed 4.6 years apart. Patient age averaged 58.2 ± 5.9 (range, 51 to 70) years at the time of index TKR and 66.5 ± 6.1 (range, 58 to 80) years at the time of bone grafting and isolated insert exchange. Body mass index (BMI) averaged 35.6 ± 3.7 (range, 29.6 to 39.1) kg/m^2. The duration of function for the index TKR averaged 8.7 ± 1.9 (range, 5.7 to 11.4) years prior to the bone grafting and isolated insert exchange procedure, and the length of follow-up time after the procedure averaged 5.1 ± 2.4 (range, 1.0 to 10.0) years. Eight patients were treated with cancellous allograft, two with demineralized bone matrix putty, and one with a mixture of both cancellous allograft and demineralized bone matrix putty.

Clinical follow-up of these 10 cases revealed no further complications in 100% of

the patients, with no reported clinical symptoms of pain and no new areas of osteolysis noted on follow-up radiographs. None of the knees have required additional surgical intervention. One patient suffered multiple long bone fractures including a periprosthetic femoral fracture 2 years later due to a motorcycle trauma but the index TKR components remained intact without need for revision. The average Knee Society score improved from 96.4 ± 5.3 (range, 85 to 100) before the bone grafting and isolated insert exchange to 98.5 ± 2.4 (range, 95 to 100) at the most recent follow up.

Detailed review of the radiographs revealed findings consistent with the criteria defined in the pre-operative surgical decision model (Fig. 4), confirming that no TKR exhibited radiolucent lines at the interface of the femoral or tibial component prior to bone grafting and isolated insert exchange. Tibial osteolytic lesions assessed on the pre-operative films were graded as small in 2 TKR, medium in 4 TKR and large in 3 TKR. Similarly, femoral osteolytic lesions were graded as medium in 2 TKR, large in 4 TKR, and absent in 4 TKR (Fig. 6 and Fig. 7). Post-operative radiographs revealed complete graft incorporation into the regions that were previously osteolytic, with an absence of radiolucent lines and no signs of component migration or loosening (Fig. 6 and Fig. 7).

Discussion

In cementless total joint replacement, periprosthetic osteolysis associated with polyethylene wear is a known complication.[24-32] Isolated exchange of polyethylene bearings in THR and TKR has been used with some success. Due to the more variable outcomes in TKR, we developed uniform pre- and intra-operative surgical decision

models to guide our selection of clinical treatment options. The criteria in the surgical decision models provided for consistent outcomes at an average of 5 years of follow up, with no additional surgical intervention required in these carefully selected patients.

Bone grafting proved useful for treating osteolytic lesions adjacent to both femoral and tibial components, with full graft incorporation effectively eliminating the lesion site and preventing recurrence at 1 to 10 years follow up. These results are more favorable than previous studies. Whiteside and Katerberg[42] performed isolated insert exchanges on 49 TKR for wear with a 6% failure rate at 3 years. In 56 TKR patients presenting with instability or polyethylene wear who were treated with isolated insert exchange, Babis, et al.[37] reported a 25% rerevision rate at a mean of three years follow-up. Engh, et al.[43] performed isolated insert exchange due to wear on 48 TKRs with 7 exchanges failing. Using isolated insert exchange and either bone grafting or cement augmentation to treat 76 TKR patients with polyethylene wear and osteolysis, Griffin, et al.[38] reported a 16.2% failure rate after a mean forty-four months. Using a surgical technique similar to the current study, Callaghan, et al.[39] reported a 4% rerevision rate in 22 patients at an average of 61 months follow up. These variable results can be partially attributed to varied inclusion criteria, especially related to joint instability.[37,38] Based on previous surgical outcomes combined with our results, the selected use of bone grafting and isolated insert exchange to treat periprosthetic osteolysis appears warranted.

This study utilizes a historical control group for comparison, which is an appropriate comparison for this study because had the femoral and tibial components been removed the residual defect would have required revision stemmed implants the

options of metal augments, structural bulk allografts, and cancellous allografts. This control group includes patients who required a revision surgery in which auto- or allograft bone grafts (structural, bulk or morselized), metal wedges, and modular components were used.[44-48] Peters, et al.[48] reported a survivorship of 75% ± 25% at 99 months of 57 revision TKR after the bone defects were excavated and treated. Cortical allograft bone was used to treat large segmental defects, while cavitary defects were filled with cancellous allograft or autograft bone.[48] Management of bone deficiency with bulk allograft had a reported survivorship of 79.4% to 83% at 8 years follow up.[46,47] An 85% survivorship was reported at an average of 4.2 years follow-up.[45] Mow and Wiedel[44] reported an 84% survivorship for a study of 13 revisions using structural allografts. The decrease in survivorship of revision TKR is well documented. This case study provides an alternate treatment option for a select subgroup of patients with areas of progressive periprosthetic osteolysis with a 100% survivorship rate at an average of 5.1 ± 2.4 (range, 1.0 to 10.0) years.

The clinical use of demineralized bone matrix and cancellous bone chips is well supported in the literature.[49,50] Although commercial preparations vary, these products deliver the necessary osteoconductive and osteoinductive components of bone to the surgical site. Bone grafting has shown success as a treatment method in both retroacetabular osteolysis in THR and periprosthetic osteolysis in TKR.[33,35,36,38,39] In the current study, treatment of osteolytic lesions included curettage and subsequent packing with bone graft material, effectively resolving the lytic progression.

Several aspects of the current study limit the ability to generalize these results.

Adhering to our pre- and intra-operative surgical decision models limited the number of cases available for inclusion. Based on our favorable outcomes in this small population, continued use and investigation of this treatment method is justified. While a single surgeon's patient data eliminated variation due to surgical technique, it is recognized that reporting results from one experienced surgeon may not represent outcomes from more wide-spread use of this technique. This method for treating progressive periprosthetic osteolysis in cementless TKR is primarily dependent on having well-fixed components at the time of revision, which in our study was enhanced through use of bone slurry at index TKR. Its effectiveness for other TKR designs or cemented TKR is unknown.

Fully incorporated grafts occurred in all ten cases in this study, including 7 large defects. These results are similar to other published results for insert exchange in TKR, ranging from 84.6% to 97% complete or near complete graft incorporation into treated osteolytic lesions.[38,39] However, considering that radiographs tend to underestimate the degree of osteolysis, it is challenging to assign a clear magnitude of the disease treated.[51] It is recognized that use of CT or MRI provide some benefit for gaining a three-dimensional perspective of the lytic defect, as recently demonstrated by others.[52,53] MRI has been shown to be more accurate and sensitive than CT for defect detection in the femur, while CT performs with better accuracy in the tibia and in defects less than 2 cm^3.[53]

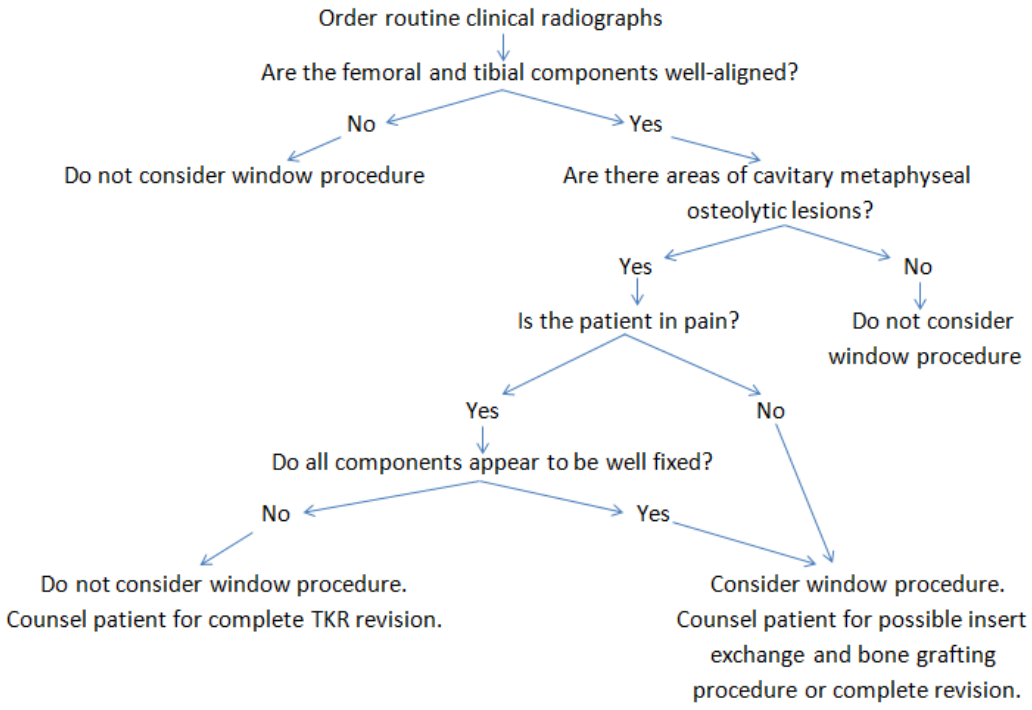

Figure 4. Pre-operative surgical decision model.

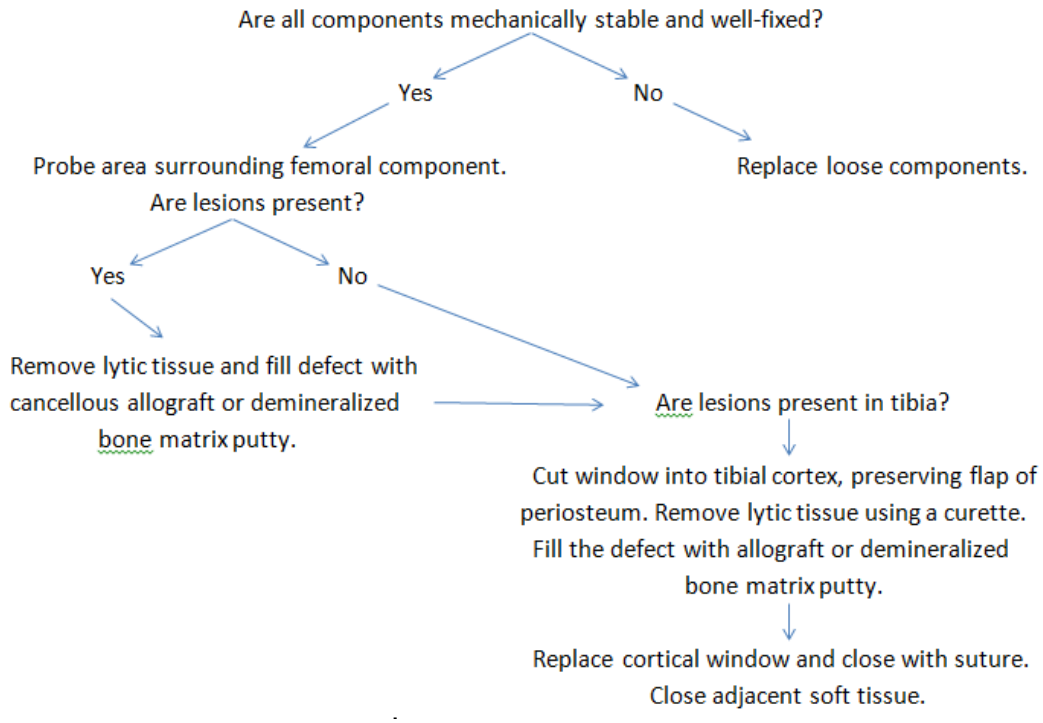

Figure 5. Intra-operative surgical decision model.

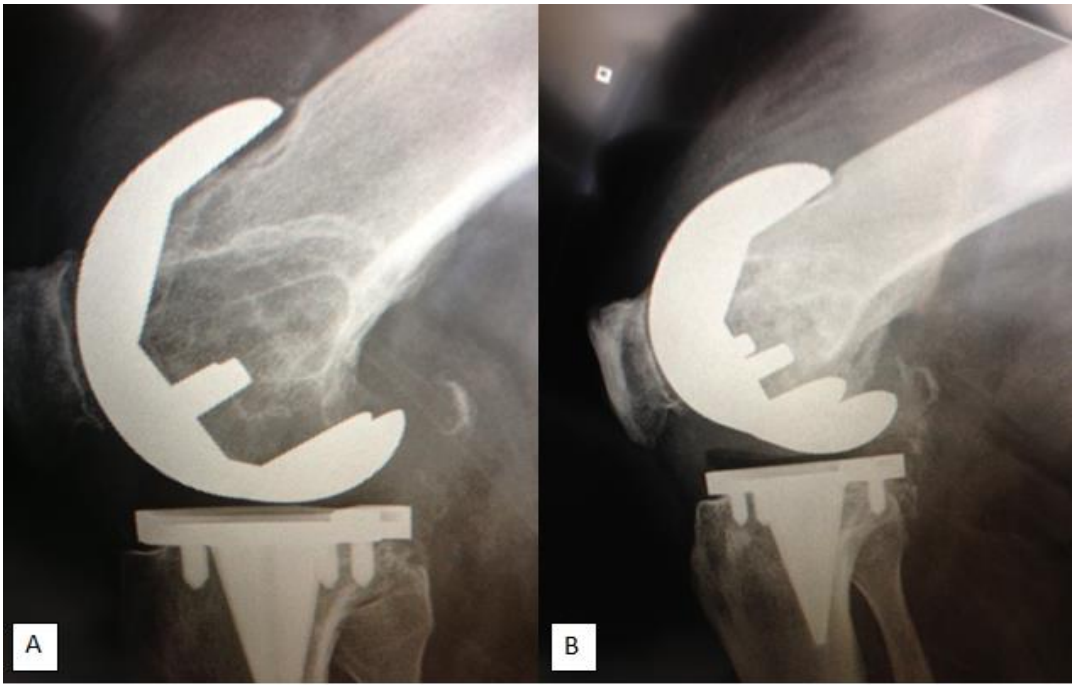

Figure 6. Radiographs of a 67 year old male who underwent bone grafting and isolated insert exchange for femoral osteolytic region. (A) Pre-revision radiograph. (B) Three month post-revision radiograph.

Figure 7. Radiographs for a 64 year old female patient who underwent bone grafting and isolated insert exchange. (A) AP view pre-revision radiograph showing osteolytic region. (B) Three months post-revision AP view radiograph.

Chapter 3
Acquire Retrieved Polyethylene Inserts and Create an Image-Based Measurement Tool with Graphical User Interface for Measuring Damage Modes

Introduction

In the event that a TKR has failed and revision surgery occurs, the explanted TKR device can be sent to a research program, such as CU-REPRO, for analysis and inclusion in future studies. Retrieval analysis is crucial to the improvement of existing TKR designs and materials. Polyethylene wear has been studied extensively, with the durability of the material contributing greatly to the success of TKR.[54] Retrieval analysis has documented the success of polyethylene in TKR while also revealing evidence of surface wear modes, surface damage, deformation, and structural failure.[54] This type of analysis provides unique insight into the effects of the physiological environment in which the TKR performed that simulations have not yet been able to replicate. In order to reduce polyethylene debris generation, changes in articular surface conformity, modular tibial locking mechanisms, and kinematic function have been made. Monitoring the effects of these changes is done through studying the bearing surface performance and design impacts on the survivorship of primary TKR.

A variety of methods exist for analyzing retrieved polyethylene inserts. Different damage modes have been identified, with both written descriptions and photographic depiction that vary depending upon the author and research institution. In order to standardize identification of different polyethylene damage modes, Harman, et al.[15]

created a study that implemented a training procedure and created an illustrated reference guide of damage modes (Damage Atlas) that are typically visualized on polyethylene bearings. One option for retrieval analysis involves a scoring system based on the worn area with a specific type of wear on the different zones of the tibial insert.[55] The articulating surface is divided into medial and lateral sides, with each side being divided into three equal zones anteroposteriorly. The worn area in each zone for each type of wear is quantified from 0 to 3, with 0 representing no damage and 3 representing greater than 50% damaged.[55] The total score is the sum of all six zones for each type of wear. Another grading system was developed to quantitate surface damage on TKR inserts. This system divides the articular surface into medial and lateral zones, with each zone being further divided into four quadrants.[56,57] Each quadrant is analyzed, with a score being assigned for a particular damage mode and all quadrants being summed. The results are then combined with patient variables, such as weight, activity level, radiographic findings, time of implantation, and results of histology, to determine correlations between clinical variables and the mechanical damage experienced by the prostheses.[56,57]

A more quantitative damage pattern analysis of the polyethylene insert portion of a TKR can be accomplished using visual recognition under low magnification using optical microscopy and photogrammetry, with resulting images digitally analyzed. There are sixteen main damage modes observed in retrieved polyethylene tibial inserts which can be readily observed at low magnification, such as in optical microscopy.[15] Ten modes derive from adhesive/abrasive or fatigue mechanisms that occur with cyclic loading, three

derive from the backside surface, and three are common artifacts as a result of surgery or manufacturing.[15] In order to ensure correct identification, use of a pictographic damage atlas is important as identification of damage modes based on descriptions obtained from literature can be inconsistent. In "A pictographic atlas for classifying damage modes on polyethylene," an illustrated reference guide of damage modes (Damage Mode Atlas) for damage observed on polyethylene was developed and a training protocol for new researchers validated.[15] Use of the Damage Mode Atlas was able to increase the rate of correct identification of damage modes and improved inter-rater reliability.

Correct identification of damage modes is the first step in quantitative retrieval analysis. After the inserts have been assessed using the unaided eye and a stereomicroscope, with the damage modes identified and manually outlined using a fine tipped marking pen, images are taken and imported. The images can then be digitally processed to obtain quantitative values for the areas of the inserts affected by the different damage modes. Harman developed a program approximately 20 years ago that effectively analyzes the inserts but lacks a user-friendly interface. In order to standardize digital processing of the inserts, a graphical user interface was developed in MatLab.

The objective of Aim 2 is to acquire polyethylene inserts that have functioned in patients and develop a custom analysis program with a graphical user interface (GUI) for completing quantitative assessments of damage patterns observed on the polyethylene inserts' surfaces. It is hypothesized that the GUI interface will provide seamless transfer between user controlled functions of image selection, calibration, digitization, damage mode identification, damage area and location measurement, damage pattern display, and

data output. In this manner, consistent and accurate assessments of damage patterns of retrieved tibial inserts can be accomplished by users without advanced training in software programming.

Materials and Methods

Retrieved TKR prosthesis explanted during revision TKR at different hospitals were accessed through archived collections within the Clemson University Retrieval of Explants Program and Registry in Orthopaedics (CU-REPRO). Conducting research on the retrieved prostheses is authorized using a protocol that was reviewed and approved by the Clemson IBC (protocol IBC2008-27). Cleaning and processing were completed following protocols based on ASTM 561-05a [REF] and ASTM F1715 [REF], and generally included formalin fixation of attached tissues, gentle cleaning with detergents, ultrasonication in methyl alcohol, and dry storage. A total of 50 TKR were obtained and assessed in this Aim (Table 1), including two different designs from two different manufacturers (Genesis II, Smith & Nephew, Memphis, TN; NexGen, Zimmer, Warsaw, IN). The materials used for the bearing couples consisted of either cobalt-chrome or oxidized zirconium femoral components and conventional or highly cross-linked UHMWPE tibial inserts with both cruciate-retaining and posterior-stabilized articular geometry.

The visual appearance and distribution of damage patterns on the articular and non-articular surfaces were evaluated using a published illustrated Damage Mode Atlas to distinguish 16 specific damage modes. These modes are recognized as typically

occurring on polyethylene bearings with low to moderate conformity and are readily observed with optical microscopy.[15] The Damage Mode Atlas includes both photographs and written descriptions (Fig. 10-11) of the 16 specific damage modes, including 10 modes consistent with adhesive/abrasive or fatigue mechanisms that can occur with cyclic loading of polyethylene bearings (Fig. 9), three modes characteristic of damage on the non-articular (backside) surface of modular bearings (Fig. 8), and three modes characteristic of common artifacts originating during surgery or manufacturing.

After undergoing training as described in the Damage Mode Atlas and demonstrating proficiency, surface damage on the tibial inserts was assessed using the unaided eye and a stereomicroscope (model Z30L, Cambridge Instruments, Cambridge, MA) fitted with a reflected light illuminator and lenses providing magnification from 7x to 30x. The distinct damage modes were identified and manually outlined using a fine tipped marking pen. Articular surfaces included the proximal insert surfaces of the medial and lateral plateaus that typically undergo direct bearing contact with femoral component. Non-articular surfaces included the distal insert surface that experiences direct contact with the tibial baseplate.

Calibrated digital images were captured for all inserts using a high resolution digital imaging system (EOS D30, Canon) with controlled illumination and photogrammetric reference scale (ABFO No. 2) for later size calibration. The images were originally captured as color JPG format with 2160 pixels by 1440 pixels per image. The horizontal and vertical resolutions were 96 dpi with a bit depth of 24 and a total size

of 8.89MB. The captured images were converted into TIFF formatted images as the TIFF format does not introduce compression into the image.

After damage evaluation and image capture, quantitative assessments were completed using custom software written in MatLab code, inclusive of two separate graphical user interfaces (GUI). The program is broken into two separately functioning GUI. The first GUI was designed to allow the user to highlight each area of damage on the implant, assign it to one of the predefined damage modes, and export data about the location and size of the damage area relevant to the center of the implant. The second GUI was designed to allow the user to complete a quantitative analysis for either single or multiple inserts, generate a visual display of damages on a single insert, and provide a visual depiction of the increasing occurrences of selected damage modes through overlaying a series of implants.

In the data collection GUI, the user imports and displays a TIFF image. A visual depiction of the process is detailed in Fig. 12. Insert rotation in the image is visually assessed and corrected by defining a posterior condylar axis (line connecting the most posterior aspects of the medial and lateral condyles) and executing the image rotation program function until that posterior axis lies parallel to a horizontal line defined by the edge of the image. After the image is rotated, the photogrammetric scale is used for image calibration for reporting accurate size dimensions, with image resolution averaging approximately 17.7 pixels/mm in the macro photographs. The user then establishes an insert-based coordinate system with the origin at the geometric center of the insert. The origin is determined by the user establishing the most extreme left, right, top, and bottom

points on the insert with the xy-coordinates from those selections being used to calculate the center. The x-coordinates of the right and left extreme points are used to determine implant width and the y-coordinates of the top and bottom extreme points are used to determine implant height. These values are later used to normalize the xy-coordinates collected during contour acquisition to a standard size. Contour acquisition is accomplished through use of a built in MatLab function called "roipoly." It allows the user to specify a polygonal region of interest within an image and returns a binary image mask and xy-coordinates. The xy-coordinates are manipulated using the implant height and width to fit the pre-determined implant size standard. The mask exports a value of 1 for each pixel contained within it. By summing the mask and multiplying it by the x and y calibrations, the area enclosed by roipoly is determined. Use of another built in MatLab function, "regionprops," allows for the determination of the centroid of the region selected by roipoly. Regionprops measures a set of properties for each connected component in the binary mask and when 'centroid' is specified, it outputs the center of mass of the region. To assign the region to a particular damage mode, the user is asked to select one of the sixteen damage modes and assign it as medial or lateral. The xy-coordinates for the damage modes and damage mode centroid locations are exported as '.mat' files. The medial centroid, lateral centroid, calibrations, and damage areas are exported as '.csv' files.

The data processing GUI has multiple functions that the user can select from and some of their uses are visually depicted in Fig. 13. There are two functions that the user can call in order to obtain a visual depiction of the damage associated with a particular

insert. One function, “Single Implant Top Surface Display,” provides a computer generated mapping of the bearing surface of the tibial insert; the second function, “Single Implant Backside Surface Display,” generates a map of the damage patterns on the surface of the tibial insert that is in contact with the metal tibial baseplate. Each damage mode is associated with a particular color that is displayed on the surface of the implant. The user is then asked if they would like to display the overall damage centroids for the insert. If yes, the user selects the centroid data and it is mapped on top of the current display. The centroid locations are calculated relative to the implant center and displayed in the table. Positive y values represent an anterior location while negative y values represent a posterior location. The positive or negative x values represent a distance from the center and, depending on the knee orientation, are either medial or lateral. In order to obtain quantitative data for an implant, the user must select the “Damage Area Percentage Calculator.” The user imports the folder containing all areas for one insert; if the user wishes to import data for multiple inserts, they may import that data as well. The program calculates the percentages of the areas in terms of: bearing surfaces in terms of total surface, total medial/lateral/total damage in terms of bearing surface, and medial/lateral/total damages in terms of bearing surface. These percentages are displayed in the table.

The accuracy of the designed programs is first evaluated by conducting a comparison test on three standard images using Image J and the developed program (Fig. 14). In order to verify the reproducibility of the program, a sample insert damage mode

was evaluated. The backside deformation region on the left of the insert was the damage mode used in the evaluation (Fig. 14).

These programs were developed to replace the analysis software previously used in the research group. This task was undertaken for several reasons, including software availability, software cost, and ease of use. The prior program was developed by Dr. Melinda Harman in 1994 in PV-Wave (version 6.21, Visual Numerics, Inc., Boulder, CO). Her program was originally applied to tibial baseplates, but evolved to include analysis of polyethylene inserts.[58-62] The program originally developed was created as it is easier to identify trends and make connections to clinical outcomes with more quantitative data. Additionally, the original program created a visual display of the damage patterns experienced by the inserts, which allows for easier interpretation of the insert damage patterns.

As PV-Wave is an array based programming language, it requires its user to have programming language knowledge in both C/C++ and Fortran code. PV-Wave software is not currently offered through Clemson University's information technology department. In order for the research group to continue quantitative polyethylene analysis, a new program that utilizes available software was needed. As MatLab is available at no charge to all university students and employees, it was selected for development of the new analysis software. Another area that development of the program focused on was ease of use. Development of a program that did not require users to have extensive programming language knowledge was crucial to its adaptation in the research group.

Results

The accuracy of the developed MatLab program was evaluated used three samples. The samples were evaluated using ImageJ and the MatLab GUI. The average areas for all three samples between the ImageJ and MatLab GUI were similar, as were the standard deviations (Table 1).

The reproducibility of the developed MatLab program was evaluated using a sample insert damage mode. The area of backside deformation on the left side of the insert was determined using both ImageJ and the MatLab GUI (Table 2). The percentage difference in the areas between the two programs was 0.09%.

Table 1. Image J and MatLab GUI Accuracy Validation Data

	ImageJ		MatLab GUI		Percentage Difference in Average Areas
Image	**Average Area**	**Standard Deviation**	**Average Area**	**Standard Deviation**	
Triangle 1	722.8	1.8	723.3	2.0	0.07
Rectangle 2	1260.4	3.7	1260.1	2.8	0.02
Triangle 3	322.9	1.5	323.6	1.3	0.22

Table 2. ImageJ and MatLab GUI Reproducibility Validation Data

	Average Area	Standard Deviation	Percentage Difference in Average Areas (%)
ImageJ	46.8	0.05	0.09
MatLab GUI	46.9	0.14	

Discussion

The developed MatLab GUIs provides for accurate, reproducible, user friendly image processing. When three sample images (two triangles, one rectangle) were evaluated using both ImageJ and the developed MatLab GUIs, there were very small percentage differences between the two values, ranging from 0.02% to 0.22%. This demonstrates the accuracy of the MatLab GUIs ability to measure areas. Additionally, the standard deviations were low and similar between the two analysis programs. In order to test the reproducibility, both programs evaluated a region of backside deformation (Fig. 14). Again, the average areas calculated were very similar, with only a percentage difference in the areas between the two programs of 0.09%. However, the MatLab program had a slightly higher standard deviation than ImageJ in this particular scenario.

The developed programs demonstrated success in image analysis and eliminated the need for users to have extensive programming knowledge. PV-Wave requires extensive knowledge of C/C++ and Fortran languages, while MatLab is a more modern programming language. Due to their development as a GUI, users lacking advanced training in software programming can still complete image processing and analysis, which allows for a greater number of lab personnel to begin conducting quantitative analysis. It is able to provide seamless transfer between user controlled functions of image selection, calibration, digitization, damage mode identification, damage area and location measurement, damage pattern display, and data output. With this GUI based program the analysis based methods originally developed by Harman, et al[15,58-62] are now more user friendly and available for use by other lab members.

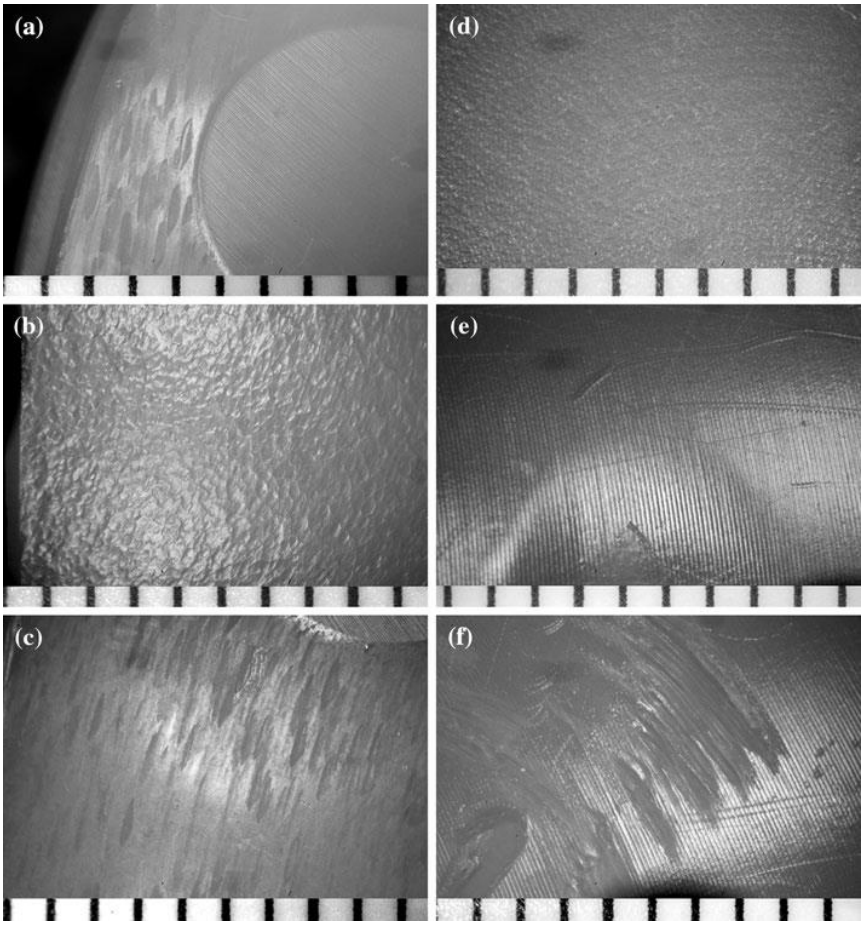

Figure 8. Damage Mode Atlas images acquired through the microscope. (A) Backside deformation with a field of stippling. (B) Dimpling. (C) Stippling. (D) Processing artifacts. (E) Visually indistinct. (F) Tool damage. [15]

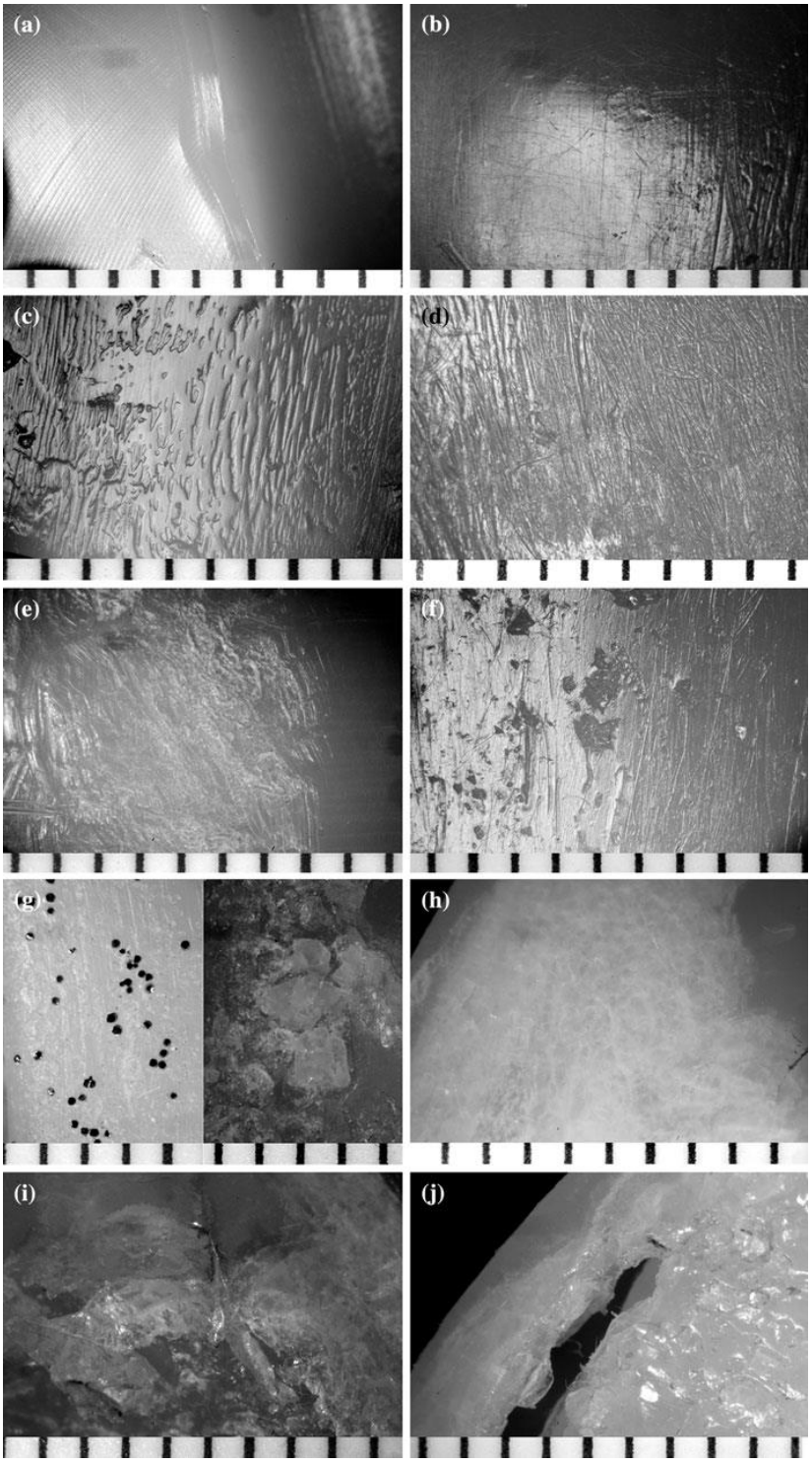

Figure 9. Damage Mode Atlas images acquired through the microscope. (A) Non-articular deformation. (B) Burnishing. (C) Striations. (D) Scratches. (E) Abrasion. (F) Pitting. (G) Embedded Debris. (H) Subsurface cracking. (I) Delamination. (J) Fracture.[15]

Damage modes	Visual appearance	Typical mechanisms
Non-articular deformation	Visualized as a permanent change in shape not associated with condylar articulation	Compressive or shear load due to contact of the metal counter-bearing in non-articular regions
Burnishing	Visualized as smooth, highly polished regions that are highly reflective of incident light	Rolling contact of the metal counter-bearing
Striations	Visualized as highly oriented, longitudinal or dispersed, smooth peaks and troughs	High friction rolling and sliding contact of the metal counter-bearing
Scratches	Visualized as thin lines in irregular or ordered directions	Sliding contact of the metal counter-bearing
Abrasion	Visualized as rough, tufted regions with limited directionality	Sliding contact with bone or third-body cement debris or rough metal
Pits	Visualized as depressions with rough surfaces and a typical diameter in the range of <1 mm up to 2 mm or greater	Material fatigue or fracture, or impressions from third body debris associated with component loosening
Embedded debris	Visualized as particles that differ in color and/or texture relative to the surrounding polyethylene surface, consistent with third-body particles of bone, cement fragments or metal	Third-body particles typically associated with component loosening or fracture
Subsurface cracking	Visualized as cracks and/or discoloration located inferior to the articular plane without surface discontinuity (rupture)	Fatigue, high sub-surface stress
Delamination	Visualized as thin layers of polyethylene material separated from the surface, with the remaining exposed material typically appearing textured and/or grossly pitted	Fatigue, high contact stress
Fracture	Visualized as complete cracks or wear-through of the polyethylene bearing, typically resulting in exposure of the metal baseplate or discontinuity of the bearing rim	Fatigue, high contact stress
Backside deformation	Visualized as permanent changes in shape typically observed around protrusions or screw holes existing on the metal baseplate	Compressive load deforming the polyethylene bearing against features on the metal baseplate
Dimpling	Visualized as uniform, nearly circular indentations approximately 100 μm in diameter that lack directionality	Compressive load deforming the polyethylene bearing against the textured metal baseplate
Stippling	Visualized as unidirectional scratches approximately 1 mm or greater in length	Motion in the shear plane between the polyethylene bearing and metal baseplate
Processing artifacts (no damage)	Visualized as highly ordered and repeating patterns consisting of linear scratches (machine marks), uniform dimpled texture (molding), or a highly glossy surface (compression molding)	Contact with tools and molds during manufacturing
Visually indistinct	Visualized as a disruption to machine marks or the original manufactured surface, but no clear damage mode can be distinguished microscopically	Infrequent contact with smooth articular surface of the metal counter-bearing
Tool damage	Visualized as symmetric pattern with sharply distinct edges, or severe singular scratches or cuts that are incongruous with the surrounding damage modes	Grasping bearing with serrated surgical clamp, prying with chisel to disengage modular bearing, or contact with sharp saw or scalpel

Figure 10. Descriptions of distinct features characteristic for each damage mode, including the visual appearance under optical microscopy and typical mechanisms potentially contributing to the damage.[15]

Damage modes	Scale	Typical location	Color change	Texture	Reflectivity
Non-articular deformation	Macro	Non-articular	Absent	Smooth	High
Burnishing	Macro/micro	Articular	Absent	Smooth	High
Striations	Micro	Articular	Absent	Rough	High
Scratches	Macro/micro	Articular/rim/non-articular	Absent	Rough	Low
Abrasion	Macro	Articular/rim/non-articular	Present (opaque)	Rough	Low
Pits	Micro	Articular	Absent	Rough	Low
Embedded debris	Macro/micro	Articular/backside	Present	Rough	Low/high
Subsurface cracking	Macro	Articular/rim/non-articular	Present (opaque)	Smooth	Low/high
Delamination	Macro	Articular/rim/non-articular	Absent/present	Rough	Low
Fracture	Macro	Articular/rim/non-articular	Absent	Rough	Low
Backside deformation	Macro	Backside	Absent	None	Low
Dimpling	Micro	Backside	Absent	Rough	High
Stippling	Macro	Backside	Absent	Rough	Low
Processing artifacts (no damage)	Macro/micro	Articular/rim/non-articular	Absent	Rough/smooth[a]	Low/high
Visually indistinct	Macro	Articular	Absent	None	High
Tool damage	Macro	Rim/non-articular	Absent	Rough	Low

[a] Processing artifacts on the original surface serve as the reference control for texture

Figure 11. Five distinguishing features for each damage mode.[15]

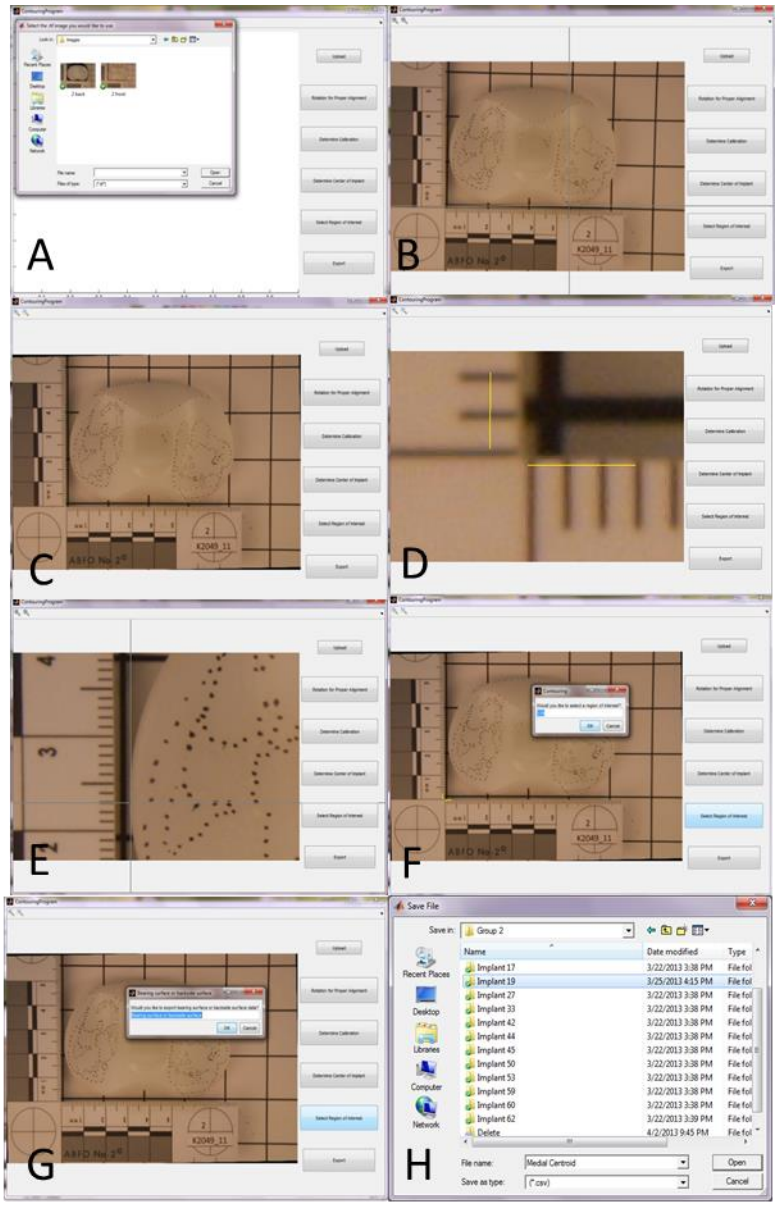

Figure 12. Image contouring GUI process. (A) Import .TIFF image. (B) Rotation of image. (C) Rotated image. (D) Calibration of image. (E) Determination of center of implant – left side point acquisition. (F) Begin contouring process. (G) Export of either bearing or backside surface. (H) Saving exported file.

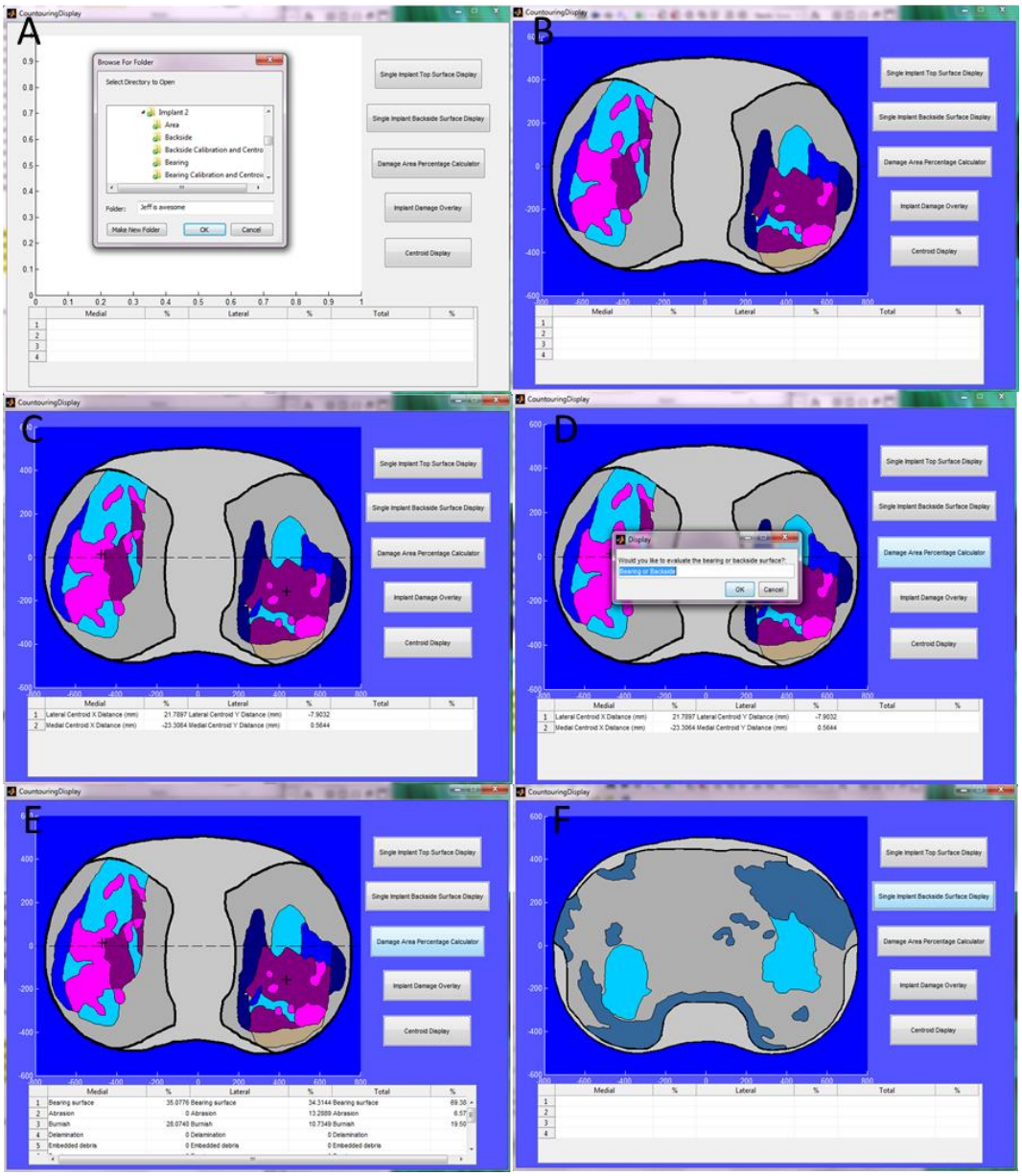

Figure 13. Display GUI process. (A) Import folder for display. (B) Display of bearing surface. (C) Centroid display with table containing centroid location. (D) Import folder for area analysis. (E) Display of calculated area percentages. (F) Backside surface damage display.

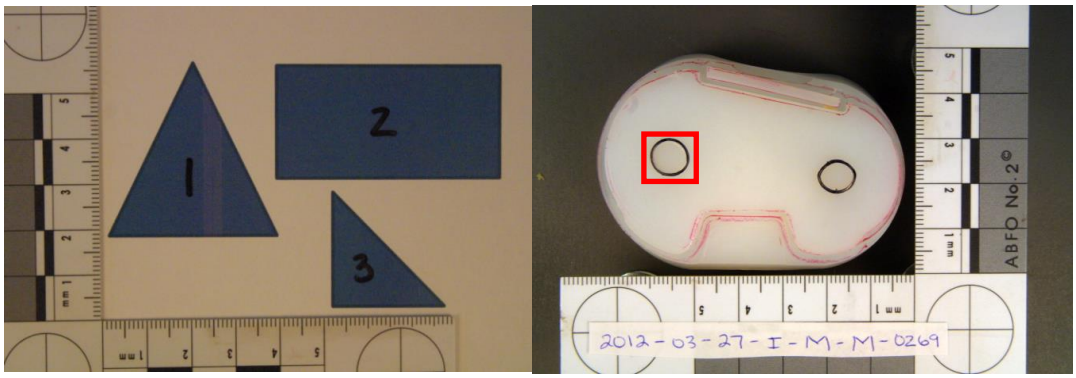

Figure 14. The image on the left is the standard used for accuracy validation. The image on the right, with the highlighted red portion, is used for reproducibility validation.

Chapter 4
Distinguish Variations in Damage Distribution Comparing TKR Designs with Different Types of Polyethylene and Different Articular Constraint

Introduction

Since the invention of TKR, changes to design in pursuit of a device with a longer lifespan have occurred. At present, TKRs can have either fixed or mobile polyethylene inserts, posterior stabilized or posterior cruciate ligament retaining, and highly cross-linked or conventional polyethylene inserts.

In a TKR the tibial insert can be either fixed to the tibial plateau or mobile. A fixed-bearing TKR is a design in which the tibial insert is locked into the metal tibial component. Different manufacturers have differing locking mechanisms for the polyethylene-tibial plateau interface. Mobile-bearing TKRs were designed as an alternative to fixed-bearing in order to reduce wear and revision rates.[63-66] Several variations in design exist to either allow rotation or translation between the femoral and tibial components. Rotations about a longitudinal axis, translation in the anterior-posterior direction, or a combination of the two were developed to allow the movements of a revised knee to more closely mimic the normal knee throughout flexion and extension. One of the primary reasons for the creation of mobile-bearing TKRs was to reduce polyethylene wear, as premature wear of the UHMWPE is one of the major causes of device failure.[55] In theory, the allowing of relative movement between the lower surface of the tibial insert and baseplate reduces the constraint force and the congruity of

the insert reduces contact stresses, leading to an overall reduction of polyethylene wear. The results showed that the amount of wear on the upper surface of the polyethylene is reduced for the mobile-bearing design when compared to the fixed-bearing design; however, the backside surface of the mobile-bearing inserts showed a higher incidence of high-grade wear patterns.[55] A retrospective analysis of prospectively collected data identified with the use of a total joint replacement registry with the purpose of comparing short-term survivorship and evaluating the risk factors for revisions of mobile-bearing compared with fixed-bearing TKRs and determined that the low contact stress mobile-bearing design TKRs had a higher risk of revision than fixed-bearing TKRs.[64]

The majority of patients are currently treated with a fixed-bearing TKR and there are two types of design for TKRs that are used to control joint stability – posterior stabilized or posterior cruciate ligament (PCL) retaining. Depending upon the patient's needs, a surgeon can choose either design. Overall, PCL retaining and posterior stabilized TKR designs have similar clinical outcomes.

Use of posterior stabilized TKRs can be dependent upon surgeon preference, availability, or the condition of the surrounding soft tissues and posterior cruciate ligament (PCL). The PCL is the strongest of the four ligaments in the knee, providing it with stability while pulling back the femur posteriorly onto the tibia during "roll-back", thereby preventing posterior translation of the tibia.[16] The removal of the PCL thus necessitates the addition of a post to the polyethylene insert that articulates with the metal cam portion of the femoral component in order to restore stability to the joint. The cam-post mechanism was developed to induce posterior femoral translation during deep knee flexion with the goal of increasing maximum knee flexion; different designs allow for

different degrees of flexion, ranging from between 20° to 65° of flexion.[17,18] One of the problems associated with TKR that posterior stabilized knees sought to overcome was that patients rarely flex the knees beyond 120° after surgery.[19] Posterior stabilized TKRs have been evaluated in terms of patient function, knee kinematics, rotational kinematics, risk of post fracture, survivorship, rates of osteolysis, range of motion, and clinical results.

Several studies have been conducted to assess the intermediate to long term results of posterior stabilized TKR. After a minimum of five years follow-up increased rates of osteolysis were reported for modular, posterior stabilized TKRs.[67] After a mean follow-up of twelve years, the rate of osteolysis was 4%, with overall excellent or good results in 89% of knees with well-fixed components and a rate of revision of 3%.[21] Impingement and wear of the post are believed to be some of the reasons for the higher rate of osteolysis.[67] Additionally, fatigue wear of the post from impingement in the trochlear groove during extension was deemed a source of abnormal stress at the cement-bone interface, cement-implant interface, and polyethylene-tibial tray interface.[67]

In order to determine the tibiofemoral kinematics, maximum flexion, and timing of the cam-post engagement in patients after posterior stabilized TKR, a dual-orthogonal fluoroscopic system was used to obtain data from an Asian population during a single leg, weight bearing-flexion.[18] The system allowed for the determination of posterior femoral translation, internal tibial rotation, and tibiofemoral contact locations. The study suggested that greater flexion may be obtained from later cam-post engagement. A sharp increase in posterior translation of the femur and tibiofemoral contact locations beyond

90° of flexion was noted just after the cam-post engagement begun and at high flexion there was a reduction in internal tibia rotation. Of note is the observation that initial cam-post contact primarily began at the medial corner of the post, explaining the reduction in internal tibial rotation as it would cause the tibia to rotate externally.[18] Suggs, et al.[18] reported that for every 0.5° increase in active flexion required 1° of cam-post engagement delay. These kinematics are design dependent and differences in the post-cam engagement mechanism will alter flexion stability and posterior femoral rollback.[68]

Preoperative and postoperative range of motion and KSS scores, incidence of manipulations, revision, survivorship analysis and radiographic data can be used to evaluate midterm clinical results of an altered posterior stabilized TKR design. The design deepened the patellar sulcus, recessed it in the femoral box, truncated the sides of the patellar flange, altered the medial-lateral and anterior-posterior radii of articulation, and increased the jump height of the femur over the tibia.[69] The KSS scores improved to 92.8 with a corresponding increase in range of motion (105° preoperative to 120° postoperative).[69] 12.3% of patients in this study required manipulation under anesthesia due to failure to achieve 90° of flexion 6 week postoperatively, but 14% of those patients suffered from postoperative complications that restricted their flexion, and less than 2% of patients required revision surgery at an average of 7 years follow-up.[69] No evidence of radiolucencies and no indications of implant loosening were noted at most recent follow-up. This particular posterior stabilized TKR design has a predicted survivorship of 97.2% at 10 years;[69] long-term durability for posterior stabilized TKR designs approaching more than twenty years of success has been noted in other survivorship analyses.[68]

In some cases, the PCL can be retained in patients and a PCL retaining TKR design is utilized. There has been some debate about whether the PCL should remain intact or be resected during the TKR procedure, with soft tissue conditions and surgeon preference playing a role in the decision making process. Some potential disadvantages associated with this design are PCL rupture, patellofemoral malalignment, and posteromedial polyethylene wear and may influence survivorship of the prosthesis.[20] Overall, PCL retaining fixed-bearing TKR designs are highly successful with the need for additional surgery occurring at approximately 0.4% per year for the first 27 years[9] and survivorship rates after 10 years at 87% to 95.7%.[20] Evaluations of PCL retaining TKR designs include analysis of long-term survival, tibial translation, maximum flexion, and anteroposterior stability.

Increased range of motion is crucial to Asian and Middle Eastern cultures, with many of their religious and lifestyle activities involving kneeling. Ginsel, et al.[70] used fluoroscopy to study the kinematics of a new PCL retaining TKR design in highly flexed postures and to determine if the kneeling position allows for greater flexion than the lunge position, the traditionally used position in the study of knee kinematics. Greater flexion was obtained in kneeling (131°) than in lunge (120°). Additionally, the new PCL retaining TKR design evaluated in this study allowed patients to have an additional average gain of 16° maximum flexion postoperatively.[70]

Anteroposterior (AP) stability has been associated with a better range of motion, clinical outcome, and device stability.[71,72] In order for the PCL to be deemed as functioning properly, the difference in the laxity or AP displacement of the knee between

the intra-operative and follow-up assessments needed to be less than or equal to 3mm. AP stability is influenced by gender, type of bearing, and age, with men, fixed-bearing, and older patients demonstrating lower laxity.[72] There is not a significant correlation between knee laxity and passive flexion; in patients with intermediate knee laxity, a trend was found toward higher passive flexion. At over 5 years of follow-up after a PCL-retaining TKR was implanted, the PCL remained correctly balanced and functional.[72] Range of motion and function two years post-operatively was evaluated to correlate it to postoperative AP movement in 100 patients broken into three groups according to the extent of AP translation. A significant difference between the three groups was noted between flexion, hyperextension, and AP stability at two years postoperation.[71] Additionally, a positive correlation was discovered between AP translation and final range of motion, with hyperextension increasing with increasing AP translation. Patients with more than 5mm of translocation had adequate range of motion and function, but when translation exceeded 10mm, there was an increased risk of hyperextension. One study hypothesized that an over 15 year follow-up study would show a survival rate for PCL retaining TKR below 90% with PCL rupture, posteromedial polyethylene wear and patellofemoral complications leading to revision.[20] Cosurvivorship was 92.5% over 17 years, with fourteen knees failing for reasons that were ranged from aseptic loosening with severe osteolysis. Guo, et al.[20] concluded that varus and valgus deformity of the operated knee could be important factors for prosthesis failure.

There is considerable debate about the use of PCL retaining or posterior stabilized TKR designs. One way in which the difference between the two was measured was

through long-term survival analysis.[73] PCL retaining TKRs had an overall survival rate of 99.7% at one year, 98.3% at 5 years, 95.7% at 10 years, 89.8% at 15 years, and 83.2% at 20 years. Posterior stabilized TKRs had overall survival rates of 99.4% at 1 year, 96.8% at 5 years, 92.2% at 10 years, and 76.5% at 15 years. Even with accounting to patient dependent factors such as age, gender, diagnosis, and deformity, PCL retaining TKRs had significantly improved survival compared to posterior stabilized designs.[73] Abdel, et al.[73] reported that an age greater than 70 years old, female sex, and a diagnosis of inflammatory arthritis are associated with increased implant survival and patients diagnosed with inflammatory arthritis have significantly greater survival.

Long-term survivorship is not the only metric used to evaluate differences in the two different articular constraints. Postoperative KSS function scores, KSS pain scores, KSS, range of motion, flexion and extension angle, and complications can also be used. A systematic review and meta-analysis of randomized controlled trials comparing posterior stabilized and PCL retaining TKRs was completed.[74] Posterior stabilized TKR designs had better range of motion and flexion angle compared to PCL retaining designs with no differences existing between the two designs for the three clinical knee scores, extension angle, complication, and prosthesis survivorship.[74] Posterior stabilized TKR had 11.1° greater range of motion than PCL retaining TKR and a 2.9° difference in flexion angle. Overall, PCL retaining and posterior stabilized TKR designs have similar clinical outcomes.

Both conventional and highly cross-linked UHMWPE are used in total knee replacements. Since the creation of the total knee replacement, multiple modifications

have been completed in an attempt to improve the functionality and life cycle of the device. Osteolysis has been associated with backside wear and tibial modularity, the polyethylene sterilization method and stock, and the design of the posterior stabilized tibial post.[21] Other factors that contribute to polyethylene debris generation and osteolysis include patient age, patient activity level, and surgical factors. Cross-linked ultra-high molecular weight polyethylene (UHMWPE) was developed to reduce volumetric wear in both hip and knee prostheses in comparison to standard UHMWPE.[22]

As with all semicrystalline polymers, UHMWPE's mechanical properties are dependent upon its chemical structure, molecular weight, crystalline organization, and thermal history, which influence wear and performance of the tibial inserts. UHMWPE is a two-phase viscoplastic solid consisting of crystalline domains embedded within an amorphous matrix.[75] The complexity at the nanoscale makes UHMWPE a composite material capable of changing over time in response to mechanical, chemical, and thermal stimuli. The mechanical properties of UHMWPE are related to its average molecular weight, which can be calculated from intrinsic viscosity measurements.[75] That viscosity is related to the bulk impact strength and abrasive wear resistance of the tibial insert. The static fracture response also depends on the molecular weight at large strains.[75]

The creation of the tibial insert from UHMWPE stock material is dependent, to a certain degree, on the desired shape. The exact methods used by total knee replacement device manufacturers are proprietary but some assumptions can be made.[75] Inserts that are relatively flat can be milled using bulk compression molded slab stock. Flat inserts can also be created from extruded rod stock that has been sliced into pucks that are milled

into the correct geometry. Tibial inserts can also be manufactured through direct compression molding of resin material. The resin is converted to a finished or semi-finished part using individual molds and, as of 1999, this method had been in use for over twenty years.[75]

The extent of different damage mechanisms on the UHMWPE tibial inserts depends not only on patient age, patient activity level, and surgical factors, but also the surface roughness of the metallic and polyethylene components. UHMWPE components "off-the-shelf" can have surface roughness values from 0.28 μm to 0.89μm.[75] Other factors that impact the polyethylene are the sterilization methods used and resulting degradation. From 1948 up until 1995, sterilization of UHMWPE was performed using gamma radiation in the presence of air.[75-77] Gamma irradiation leads to the creation of long-lived free radicals which react with oxygen. This ultimately results in progressive oxidation, breaking of polymer chains, alteration of crystalline portions of the polymer, and deterioration of mechanical properties.[76] By 1998 all of the major manufacturers of total joint replacement devices had switched to either sterilization using gamma irradiation in a reduced oxygen environment, such as nitrogen gas, or sterilizing without ionizing radiation, using either ethylene oxide or gas plasma.[75,77]

Cross-linking UHMWPE has been shown to improve abrasion and delamination resistance, although the process of cross-linking the polyethylene may reduce some of its mechanical properties.[75,77] This method of treatment was clinically introduced starting in 1998 with the intention of reducing wear, reducing the incidence of revision resulting from osteolysis, and to reduce oxidation, which had been associated with short-term

clinical failures.[78] There are two primary ways of cross-linking UHMWPE: annealing after irradiation or remelting the polyethylene after irradiation.[22,78] Annealing UHMWPE creates free radicals which can lead to late oxidation of the polyethylene. Remelting removes the free radicals from the polyethylene but reduces its fatigue strength. Using ionizing radiation followed by thermal treatment to crosslink the polyethylene and eliminate free radicals helps to increase the inserts abrasive wear resistance.[77] Irradiation creates both crosslinks and residual free radicals, but the free radicals are trapped in the crystalline domains. By heating after irradiation, the polyethylene crystalline states become amorphous which allows the free radicals to combine with one another.[77]

Traditionally, UHMWPE is cross-linked through gamma or electron-beam radiation of a ram-extruded bar stock or compression-molded sheet polyethylene at a dose greater than 4 MRads.[23] Thermal treatment eliminates or reduces free radicals while enhancing the saturation of cross-linking. Implants can then be machined from the treated UHMWPE. If a manufacturer prefers remelting, they will typically sterilize the insert using ethylene oxide gas or gas plasma techniques; if annealing is preferred, then conventional gamma sterilization in an inert environment is used for sterilization.[23]

As the goal of cross-linking was to reduce the amount of volumetric wear, it is has been the focus of several papers. One study comparing the two different types of polyethylene concluded that cross-linking was able to reduce wear by up to 92% following three million elliptical cycles. However, the reduction in wear is accompanied by reduction in mechanical properties, such as ultimate tensile strength, yield strength, elongation/ductility and toughness.[23] The majority of clinical research that has been

conducted with respect to highly cross-linked UHMWPE has taken place in total hip replacements as it was only introduced in total knee replacement starting in 2001.[79] After more than a decade of use, knowledge of in vivo damage mechanisms and oxidative stability of remelted highly cross-linked polyethylenes is still lacking. MacDonald, et al.[79] investigated the damage mechanisms and oxidative stability of remelted highly cross-linked UHMWPE in a series of retrieved tibial inserts. Oxidation was lower in the highly cross-linked group than in the gamma inert group of inserts, but the highly cross-linked group did have measurable levels of oxidation at the bearing surface.[79] Additionally, the inserts showed mainly abrasive and adhesive wear as opposed to fatigue mechanisms. Overall, remelted polyethylene has very low residual free radical but has compromised physical properties compared to conventional polyethylene. Anneal polyethylene has a higher density of free radicals but has closer physical properties compared to conventional polyethylene.

The objective of Aim 3 is to use the image-based measurement tool developed in Aim 2 to assess damage patterns occurring on the retrieved polyethylene tibial inserts with different types of polyethylene, namely conventional and highly cross-linked UHMWPE, and on tibial inserts with different types of articular constraint, namely cruciate-retaining and posterior-stabilized. It is hypothesized that tibial inserts fabricated from highly cross-linked UHMWPE will have damage modes occurring at different frequencies compared to the conventional UHMWPE inserts. It also is hypothesized that tibial inserts with the posterior stabilized constraint will have damage patterns located

more posterior than the inserts with cruciate retaining constraint.

Materials and Methods

Patient demographics were obtained from existing CU-REPRO records for the 50 retrieved TKR acquired in Aim 2. There were 26 males, 22 females, and 2 unknown gender with an average body mass index of 31.0 + 6.5 (range, 18.1 to 46.5) kg/m2 and an average age at the time of revision of 63.3 + 10.1 (range, 35 to 79) years. Duration of function averaged 3.4 + 3.8 (range, 0.1 to 20) years. Reasons for revision included instability (5), instability with pain (1), infection (14), stiffness (6), stiffness with pain (1), loosening (8), loosening with osteolysis (1), patellar complications (3), synovitis with recurrent effusion (1), peri-prosthetic fracture (1), and unknown (8).

Using the retrieved bearing materials and articular geometry acquired in Aim 2, several different comparison groups were established to evaluate the damage patterns occurring on inserts fabricated from conventional and highly cross-linked UHMWPE and having different articular constraint, namely cruciate-retaining and posterior-stabilized.

Two comparison groups were used to assess the performance of the conventional and highly cross-linked UHMWPE. The first comparison group (Compare UHMWPE 1) provided for assessment of different UHMWPE materials from a single manufacturer's design (Genesis II) comparing highly cross-linked UHMWPE posterior stabilized inserts articulating with oxidized zirconium femoral components (n = 12) versus conventional UHMWPE posterior stabilized inserts articulating with cobalt chromium alloy femoral components (n = 12). The second comparison group (Compare UHMWPE 2) provided

for assessment of different UHMWPE materials from both included manufacturers, comparing all highly cross-linked posterior stabilized inserts (n = 14) with all conventional posterior stabilized inserts (n = 26).

Three comparison groups were used to assess the performance of the cruciate-retaining and posterior-stabilize articular constraints. The first comparison group (Compare CONSTRAINT 1) provided for assessment of different articular constraint from both included manufacturers, comparing all posterior stabilized inserts (n = 40) with all cruciate retaining inserts (n = 10). The second comparison group (Compare CONSTRAINT 2) provided for assessment of different articular constraint from a single manufacturer's design (Genesis II), comparing posterior stabilized inserts (n = 25) with cruciate retaining inserts (n = 10). The third comparison group (Compare CONSTRAINT 3) provided for assessment of different articular constraint including only a single highly cross-linked design (Genesis II) having either posterior stabilized inserts (n=12) or cruciate retaining inserts (n=9).

As discussed in Aim 2, articular damage patterns were identified according to the Damage Mode Atlas using an optical stereomicroscope and photogrammetry. The photogrammetry was completed using published methods and custom analysis software written in MatLab. The purpose of this aim is to identify differences in frequency of damage modes and damage location in all comparison groups which is accomplished using the methodology developed in Aim 2.

Table 3. Patient Demographics for Comparison Groups

Compare Group	*In Vivo* Time (years)	Gender	Average Age (years)	BMI	Revision Reasons
UHMWPE 1	3.1 ± 2.7	10 F, 12 M, 2 U	61.5 ± 11.4	31.1 ± 6.9	Stiffness (6), patellar complications (1), loosening (4), loosening with osteolysis (1), infection (7), instability (2), synovitis with recurrent effusion (1), unknown (2)
UHMWPE 2	3.7 ± 4.1	28 F, 19 M, 2 U	63.2 ± 10.6	31.1 ± 6.8	Stiffness (6), stiffness with pain (1), patellar complications (2), loosening (7), loosening with osteolysis (1), infection (10), instability (2), synovitis with recurrent effusion (1), unknown (4)
CONSTRAINT 1	3.4 ± 3.8	22 F, 26 M, 2 U	63.3 ± 10.1	31.0 ± 6.5	Instability (5), instability with pain (1), infection (14), stiffness (6), stiffness with pain (1), loosening (8), loosening with osteolysis (1), patellar complications (3), synovitis with recurrent effusion (1), peri-prosthetic fracture (1), unknown (8)
CONSTRAINT 2	2.8 ± 2.5	24 F, 19 M, 1 U	62.2 ± 10.5	31.0 ± 6.3	Instability (5), infection (11), stiffness (6), loosening (4), loosening with osteolysis (1), patellar complication (2), synovitis with recurrent effusion (1), unknown (4)
CONSTRAINT 3	2.5 ± 1.5	9 F, 10 M, 1 U	60.5 ± 10.9	30.9 ± 6.5	Stiffness (4), infection (7), loosening (1), patellar complications (2), instability (4), unknown (3)

Results

The results for Compare UHMWPE 1, Compare UHMWPE 2, Compare CONSTRAINT 1, Compare CONSTRAINT 2, and Compare CONSTRAINT 3 are summarized in Tables 4-8.

When evaluating damage centroid locations, Compare CONSTRAINT 1 and CONSTRAINT 2 did not yield any statistically significant differences. For Compare CONSTRAINT 2, although not statistically significant, the cruciate retaining inserts were located closer to the center line of the inserts than the posterior stabilized inserts for the medial damage centroid (ANOVA, P = 0.387) and more posterior for the lateral damage centroid (ANOVA, P = 0.304) than the posterior stabilized counterparts. Compare CONSTRAINT 3 did not have a statistically significant difference between the medial damage centroid location (ANOVA, P = 0.745) but there was a statistically significant difference between the lateral damage centroid location (ANOVA, P = 0.020). The lateral damage centroid location for the cruciate retaining inserts was located anterior while the posterior stabilized inserts lateral damage centroid location was posterior.

The statistical analysis of the data set for Compare CONSTRAINT 3 (n = 21) showed that there was a difference in the average medial damage percent (ANOVA, P = 0.061) and a statistically significant difference in the average lateral damage percent (ANOVA, P = 0.036). The posterior stabilized inserts (n = 12) had less medial and lateral damage than the PCL retaining inserts. When all Genesis II TKR designs were included (Compare CONSTRAINT 2, n = 35), there was no statistically significant differences in the medial and lateral damage percentages. The group was further expanded to include all

inserts (Compare CONSTRAINT 1, n = 50) and no statistically significant differences were found between damage percentages.

When evaluating average damage percentages, Compare UHMWPE 1 had a difference in the average medial damage percentage with conventional polyethylene inserts sustaining greater amounts of damage (ANOVA, P = 0.051). The highly cross-linked inserts showed less medial bearing surface damage. There was a statistically significant difference in the lateral damage percentages (ANOVA, P = 0.033), with the lateral damage on the highly cross-linked polyethylene inserts averaging less damage than the conventional inserts. Compare UHMWPE 2 showed a statistically significant different in the medial damage percentage (ANOVA, P = 0.009) and the lateral damage percentage (ANOVA, P = 0.014), with the averages being summarized in Table4 and Table 5.

The frequency and percent area affected by the damage modes for Compare UHMWPE 1 and Compare UHMWPE 2 are summarized in Tables 9 - 10.

Table 4. Compare UHMWPE 1 Results Summary

Group	Feature	n	Medial %	Lateral %	Medial Centroid (mm)	Lateral Centroid (mm)
Compare UHMWPE 1	Cross-linked with OxZr	12	43.2 ± 14.6	41.1 ± 14.9	-1.1 ± 3.9	0.0 ± 3.0
	Conventional with CoCr	12	55.2 ± 14.0	58.9 ± 22.6	-1.7 ± 2.1	-2.3 ± 2.1

Table 5. Compare UHMWPE 2 Results Summary

Group	Feature	n	Medial %	Lateral %	Medial Centroid (mm)	Lateral Centroid (mm)
Compare UHMWPE 2	Cross-linked with OxZr	14	45.1 ± 18.5	47.7 ± 21.7	-1.9 ± 4.6	-0.2 ± 2.8
	Conventional with CoCr	26	62.9 ± 20.3	64.1 ± 17.6	-2.0 ± 2.5	-2.8 ± 2.2

Table 6. Compare CONSTRAINT 1 Results Summary

Group	Feature	n	Medial %	Lateral %	Medial Centroid (mm)	Lateral Centroid (mm)
Compare CONSTRAINT 1	Posterior Stabilized	40	56.7 ± 21.3	58.3 ± 20.5	-2.0 ± 3.3	-1.9 ± 2.7
	PCL Retaining	10	58.7 ± 26.1	55.5 ± 18.8	-0.3 ± 3.6	-2.2 ± 2.4

Table 7. Compare CONSTRAINT 2 Results Summary

Group	Feature	n	Medial %	Lateral %	Medial Centroid (mm)	Lateral Centroid (mm)
Compare CONSTRAINT 2	Posterior Stabilized	25	49.2 ± 15.3	50.0 ± 20.8	-1.4 ± 3.1	-1.1 ± 2.8
	PCL Retaining	10	58.7 ± 26.1	55.5 ± 18.8	-0.3 ± 3.6	-2.2 ± 2.4

Table 8. Compare CONSTRAINT 3 Results Summary

Group	Feature	n	Medial %	Lateral %	Medial Centroid (mm)	Lateral Centroid (mm)
Compare CONSTRAINT 3	Posterior Stabilized	12	43.2 ± 14.6	41.1 ± 13.9	-1.1 ± 4.0	0.0 ± 3.0
	PCL Retaining	9	61.2 ± 26.5	57.6 ± 18.6	-0.5 ± 3.8	-2.8 ± 1.6

Table 9. Compare UHMWPE 1 Frequency and Area Affected Percentages

UHMWPE 1	Highly Cross-linked (n = 12)		Conventional (n = 12)	
Damage Mode	**Frequency**	**Area Affected (%)**	**Frequency**	**Area Affected (%)**
Abrasion	8	1.6 ± 2.2	8	2.4 ± 2.5
Burnish	12	21.6 ± 10.9	12	22.3 ± 12.7
Embedded Debris	0	0	1	3.0
Non-articular Deformation	2	3.4 ± 1.1	1	16.29
Pit	7	3.2 ± 4.5	10	17.3 ± 20.7
Scratch	10	10.3 ± 13.3	10	14.6 ± 15.5
Striation	8	12.6 ± 9.2	6	16.1 ± 8.0

Table 10. Compare UHMWPE 2 Frequency and Area Affected Percentages

UHMWPE 2	Highly Cross-linked (n = 14)		Conventional (n = 26)	
Damage Mode	**Frequency**	**Area Affected (%)**	**Frequency**	**Area Affected (%)**
Abrasion	8	1.6 ± 2.2	15	3.8 ± 3.7
Burnish	14	26.5 ± 16.2	22	16.8 ± 12.0
Embedded Debris	0	0	9	5.1 ± 10.1
Fracture	0	0	1	1.7
Non-articular Deformation	2	3.4 ± 1.2	1	16.3
Pitting	9	2.7 ± 4.0	24	22.4 ± 23.8
Scratch	12	11.1 ± 12.5	22	20.4 ± 20.3
Striation	8	12.6 ± 9.2	11	12.4 ± 9.2

For Compare UHMWPE 1, both the highly cross-linked and conventional posterior stabilized Genesis II inserts experienced abrasion, burnishing, non-articular deformation, pitting, scratching, and striation and the conventional polyethylene inserts also had embedded debris. The highly cross-linked inserts had a greater frequency of burnish, non-articular deformation and a lower frequency of pitting than the conventional polyethylene. The area percentages with the burnish damage mode were not significantly different despite the difference in frequency. Although the non-articular deformation occurred at a slightly higher frequency, it occurred in an average lower percentage overall; the same is true for the striation damage mode. Not only was the frequency of pitting lower in the highly cross-linked inserts but it also impacted a dramatically smaller percentage of the area. The total damage sustained by the inserts in Compare UHMWPE 1 was greater in the conventional polyethylene inserts than the highly cross-linked inserts.

Expanding the group to include all posterior stabilized inserts that are either highly cross-linked or conventional (Compare UHMWPE 2, n = 40) results demonstrate that highly cross-linked inserts experience a greater percentage of inserts affected by burnishing, scratching, and striation and a lower percentage of inserts are affected by abrasion and pitting. PCL retaining inserts have embedded debris, fracture, and non-articular deformation, which the highly cross-linked inserts in this series did not experience. Not only did the highly cross-linked inserts experience a higher frequency of burnishing, but the percentage of the area affected was also greater. The frequency of scratching was only slightly greater for highly cross-linked inserts but the area percentage

impacted by the damage was smaller. The area percentage affected by striation was similar between the two polyethylene types despite the damage occurring more frequently in the highly cross-linked insert grouping. Slightly fewer highly cross-linked inserts were affected by abrasion than in the conventional polyethylene group and they experienced the damage in a lower average area percentage. Not only did pitting occur less frequently in the highly cross-linked polyethylene inserts, it also impacted a significantly lower average area percentage. The average overall area impacted by damage was significantly lower for highly cross-linked than in conventional polyethylene inserts.

Statistical analysis of the data sets showed that for Compare UHMWPE 1 ($n = 24$) there was not a statistically significant relationship between material type and medial bearing surface damage location but there was a statistically significant difference (ANOVA, $P = 0.035$) between the two materials and the lateral bearing surface damage location. When the group was expanded to include all posterior stabilized inserts (Compare UHMWPE 2, $n = 40$), there was again no statistically significant difference in the medial damage location but a statistically significant difference (ANOVA, $P = 0.003$) in the lateral location.

Discussion

Posterior stabilized TKRs are designed to allow for patients to have a greater range of motion. In one study, posterior stabilized TKR had 11.1° greater range of

motion than PCL retaining TKR and a 2.9° difference in flexion angle.[74] For PCL retaining TKR designs, greater anteroposterior (AP) stability has been associated with a better range of motion.[71] Compare CONSTRAINT 1, CONSTRAINT 2, and CONSTRAINT 3 were used to determine if a relationship between articular constraint and overall damage location existed.

For Compare CONSTRAINT 3, there is a statistically significant difference in the lateral damage centroid location between the Genesis II highly cross-linked, posterior stabilized TKR inserts and the Genesis II highly cross-linked, cruciate retaining TKR inserts. The lateral damage centroid location for the cruciate retaining inserts was located slightly anterior while the posterior stabilized inserts lateral damage centroid location was posterior. The group was expanded to include all Genesis II posterior stabilized and PCL retaining inserts (Compare CONSTRAINT 2) and the statistical significant difference in the lateral damage centroid location was lost. Although not statistically significant, the PCL retaining inserts were located closer to the center line of the inserts than the posterior stabilized inserts for the medial damage centroid (ANOVA, $P = 0.387$) and more posterior for the lateral damage centroid (ANOVA, $P = 0.304$) than the posterior stabilized counterparts. When all posterior stabilized and PCL retaining insert lateral damage locations were analyzed, no statistical significance was found. The medial damage centroid location was more posterior in the posterior stabilized inserts than in the PCL retaining inserts (ANOVA, $P = 0.181$). In both constraint designs the lateral damage centroid was located posteriorly to the center of the insert.

Analysis of Compare CONSTRAINT 1, CONSTRAINT 2, and CONSTRAINT 3

showed that the medial damage location was retained more centrally in the PCL retaining inserts than in the posterior stabilized inserts. The lateral damage location was statistically significantly different in one of the three groupings, with the posterior stabilized design having a more central lateral damage location. In the Compare CONSTRAINT 3 posterior stabilized inserts, the medial damage centroid location was more posterior than the lateral damage centroid location while for the PCL retaining inserts the opposite was found. The posterior stabilized inserts in Compare CONSTRAINT 1 and CONSTRAINT 2 also had the medial damage centroid located more anteriorly than the lateral damage centroid, although the difference between the two locations was reduced. The PCL retaining inserts in Compare CONSTRAINT 1 and CONSTRAINT 2 also had the average lateral damage centroid located more posteriorly than the medial damage centroid.

Very few studies have been published that contain quantitative information related to the damage centroid location. In one study, PCL retaining inserts were evaluated with the damage centroid locations being included.[61] The study had three groupings of PCL retaining inserts: a retrieval group, a simulated walking group, and a simulated walking and stair group. The retrieval group's medial damage centroid location was 0.7 ± 2.9 mm anterior and lateral damage centroid location was 1.5 ± 3.2 mm posterior ($P = 0.112$). The simulated walking group's medial damage centroid location was 3.0 ± 0.8 mm anterior and lateral location was 0.0 ± 0.6 mm anterior ($P = 0.062$).[61] The simulated walking and stair group's medial damage centroid location was 2.3 ± 0.6 mm anterior and lateral damage centroid location was 2.3 ± 0.4 mm posterior ($P < 0.001$).

All three comparison groups used in this aim had the medial damage centroid located posterior to the center of the implant, which contrasts significantly with all three groups from the study which had the medial damage centroid location anterior. Two of the three groups from the Harman, et al[61] study had the lateral damage centroid located posteriorly, which the comparison groups in this aim are in agreement with. The comparison groups lateral damage centroid location ranged from 2.197 mm to 2.768 mm posterior, which includes the simulated walking and stair group lateral damage centroid location. The retrieval group from that study had the lateral damage centroid located slightly more anteriorly (1.5mm posterior) than the inserts in the comparison groupings. This could be attributed to the relatively short *in vivo* lifespan of the comparison groupings inserts.

No studies contained quantitative data concerning the damage centroid locations for posterior stabilized TKR inserts; however, many studies have published information regarding anterior-posterior contact ranges for medial and lateral condyles, the magnitude of axial rotation of the femur relative to the tibia, and location of center of contact on the medial and lateral condyles throughout a given activity.[80-83] These values will be used to help determine if the damage centroid location values obtained in this aim lie within the expected regions.

Under fluoroscopy, posterior stabilized inserts averaged 13.5 ± 2.5 mm posterior femoral contact point with weight bearing deep knee flexion and had an average of -5.2° ± 3.8° of tibial external rotation.[83] A second fluoroscopy study demonstrated that posterior stabilized inserts have an average range of axial rotation of 6.7° ± 2.2°, which is smaller than PCL retaining inserts experienced (9.4° ± 3.6).[80] When posterior stabilized

inserts were evaluated using three-dimensional radiological images, it was determined that there is a relatively symmetrical posterior femoral translation during flexion with a mean of 6.4 mm and 6.5mm for the medial and lateral condyles, respectively, and overall tibial internal rotation of 3.0°.[82]

Data in this aim suggests that the more posterior damage patterns centroid location on the posterior stabilized inserts, especially on the lateral plateau, reflect reduced internal-external rotational motion of the TKR during flexion and extension range of motion in daily activities. This suggestion is supported by the reduction in overall tibial internal rotation reported by Delport, et al.[82] and Banks, et al.[80]. When looking at the medial and lateral damage centroid locations for all three comparison groups, there is a greater difference between locations for PCL retaining inserts than for the posterior stabilized inserts. This is consistent with the results of a Banks and Hodge[80] study, in which it was determined that there is a relatively symmetrical posterior femoral translation during flexion with a mean of 6.4 mm and 6.5mm for the medial and lateral condyles. Similarly, it is also possible that the lateral damage centroid location is kept more central in posterior stabilized TKR designs because the central polyethylene post projecting superior into the joint space and engaging the femoral cam provides greater constraint than the cruciate retaining design. In contrast, if the PCL was damaged during the TKR surgery, or the PCL loses patency during patient aging, this soft tissue constraint is lost for cruciate retaining TKR and greater femoral translation on the UHMWPE articular surface would be expected. The large standard deviations associated with the damage centroid location raise the question of the strength of the results. In order to

reduce the standard deviation and strengthen the results, additional inserts will need to be included in future studies.

There were significant differences in damage areas when the designs with different articular constraints were compared. The average medial damage area was 43.2% ± 14.6% for posterior stabilized inserts and 61.2% ± 26.5% for cruciate retaining inserts (ANOVA, P = 0.061). The average lateral damage percentages were statistically significantly different between the two articular constraints, at 41.1% ± 14.9% for posterior stabilized inserts and 57.6% ± 18.6% for cruciate retaining (ANOVA, P = 0.036). These results support knee kinematics studies which document greater femoral translations occurring on cruciate retaining TKR compared to posterior stabilized TKR.[84]

Cross-linked UHMWPE was developed in order to reduce volumetric wear.[22] The majority of clinical research that has been conducted with respect to highly cross-linked UHMWPE has taken place in total hip replacements.[79] *In vitro* studies have been the primary source of information related to wear of highly cross-linked inserts as the material was introduced in TKR starting in 2001.[79] After more than a decade of use, knowledge of *in vivo* damage mechanisms and oxidative stability of remelted highly cross-linked polyethylene is still lacking. It is important to note than the *in vivo* lifetime of the inserts used in this research is relatively short when compared to other tibial insert damage analysis studies, with these inserts having an average lifespan between three to four years.

The results of this work showed that there was an almost 18% decrease in damage areas in the medial bearing surface and just over 16% decrease in damage areas in the

lateral bearing surface, for an average overall reduction in damage areas of 33.8%. This reduction in damage areas contrasts with published results, which reported that no statistically significant difference was seen between cross-linked and conventional inserts in terms of total surface wear in simulator studies.[85-87] It is possible that the differences in conditions experienced by the inserts (*in vivo* versus simulator) could explain the differences in damage areas. The predominate damage modes on the inserts consisted of scratching, burnish, and striation, with pitting present but no delamination. In the study comparing different TKR designs and materials the predominant wear patterns consisted of scratching, abrasion, and burnishing, and no areas of severe pitting and delamination were reported.[85]

In Compare UHMWPE 1, the highly cross-linked polyethylene inserts were affected by abrasion as frequently as the conventional polyethylene inserts and experienced similar area percentages associated with it. In Compare UHMWPE 2, slightly fewer highly cross-linked inserts were affected by abrasion than in the conventional polyethylene group and they experienced the damage in a lower average area percentage. Crosslinking UHMWPE has been shown to improve abrasion resistance, with knee simulators demonstrating marked reductions in adhesive/abrasive wear compared to conventional polyethylene inserts.[75,77,88] Studies comparing the amount of irradiation an insert is subjected to and its resulting effects on abrasive and adhesive wear have shown that with increased radiation-induced cross-linking, adhesive and abrasive wear resistance increases, up to 100 kGy.[89]

"Walking" tests in knee simulators that showed wear scars included burnishing,

deformation, striations, and some scratches on both highly cross-linked and conventional UHMWPE TKR inserts.[90] In the Genesis II TKR model, highly cross-linked polyethylene inserts experience the same frequency of striation as did the conventional polyethylene but it experienced it in an average lower area percentage. When all posterior stabilized TKR inserts were evaluated (Compare UHWMPE 2), the area percentage affected by striation was similar between the two polyethylenes despite the damage occurring at a higher frequency in the highly cross-linked inserts. Asano, et al.[89] conducted testing to determine the effects of cross-linking polyethylene for TKR inserts on wear performance and determined that as the radiation dose increased, striations occurred less frequently. The greater frequency of striations on highly cross-linked inserts in Compare UHMWPE 2 could be attributed to the small population size.

Another point of difference between highly cross-linked and conventional inserts is the frequency and area percentages affected by pitting. The frequency of pitting was lower in the highly cross-linked polyethylene inserts in both Compare UHMWPE 1 and UHMWPE 2, with significantly lower average area percentages experiencing the damage. A study using retrieved conventional and highly cross-linked polyethylene TKR inserts and determined that the inserts showed primarily abrasive and adhesive wear as opposed to fatigue mechanisms, such as pitting.[77,79] However, it must be noted that revision for loosening (9 inserts) was much more common among the conventional UHMWPE inserts (8 inserts) compared to the highly cross-linked UHMWPE inserts (n = 1), and this revision reason is a known contributor to pitting damage due to the presence of cement debris generated during component loosening. In any case, very little fatigue-related

damage was noted in all insert groups, which likely reflects their relatively short duration (less than 5 years) of function.[91]

Statistically significant differences were found in the lateral damage centroid location in both Compare UHMWPE 1 and UHMWPE 2. Differences in damage centroid location were not expected as all inserts evaluated were of the same articular constraint design (posterior stabilized). In both comparison groups, the lateral damage centroid was located significantly more posteriorly in the highly cross-linked polyethylene inserts than in the conventional polyethylene inserts. Possible reasons for this could include abnormalities in alignment, rotation, or gait of the patients. Additionally, the lateral portions of the inserts in both Comparison Groups 3 and 4 had slightly larger average area percentages experiencing damage.

It is recognized that these studies have several notable limitations. First, the number of inserts used for these comparison studies were small, reducing the statistical power considerably. Also, damage occurring in TKR is highly multi-factorial, requiring additional details about patient factors and surgical factors be included in the analysis models. Oxidation and other measures of UHMWPE degradation were not completed, nor were detailed analyses completed for the femoral component bearing surface. Finally, TKR designs from only two manufacturers were included in these studies, restricting how broadly these findings can be generalized to all TKR design. Acquisition of additional TKR retrievals is ongoing, and the techniques developed in this thesis are highly applicable for data collection in a larger study.

Chapter 5
Conclusions and Recommendations

In Aim 1, a series of 10 TKR with progressive periprosthetic osteolysis around well-fixed and well-aligned components that were treated with curettage of the osteolytic lesions, bone grafting of the resultant defect, and polyethylene insert exchange demonstrated excellent results at an average of 5 years follow up with no cases requiring rerevision surgery. The senior surgeon participating in that study continues to selectively use this approach and recommends incorporating the surgical decision models (Fig. 4-5) at the time of revision TKR. However, if this approach is to be utilized, the inclusion criteria outlined must be strictly followed.

While TKR offers patients a chance to improve their mobility, it is not successful in every case. There are many known complications associated with TKR and those complications can have devastating results, with some patients requiring multiple revision surgeries or fusion of the joint. Due to the decrease in survivorship associated with complete TKR revision, combined with the increasingly younger patient population undergoing TKR, alternative methods are a necessity. By closely monitoring the bone condition surrounding the joint replacement, completing follow-up, and assessing the patient, some cases of peri-prosthetic osteolysis can be discovered that fall within the inclusion criteria outlined in Aim 1. Bone grafting and isolated insert exchange represents a viable, less severe, surgical treatment option than total TKR revision.

In order to validate this method, further research evaluating its long-term survivorship with a larger sample size is crucial. As the senior surgeon is continuing

selective use of this approach, the sample size is increasing. Long term follow-up of the original patient series is recommended to determine survivorship of the pre- and intra-operative surgical decision models success. Once the surgical decision models have been verified with a larger sample size and longer follow-up time, additional surgeon utilization of the surgical decision models would provide valuable data to determine wide spread use success.

The development of the MatLab GUIs for the second aim allows for a user of any skill level to accurately analyze digital images of retrieved TKR polyethylene inserts. The user interface eliminates the need for detailed knowledge of computer coding. The GUIs provides for accurate, reproducible, user friendly image processing. It is comparable to results obtained using ImageJ software in terms of area calculations but surpasses ImageJ in its ability to create computer generated images depicting damage patterns and location, determination of damage centroid location, and calculations of damage area percentages. The GUIs provide seamless transfer between user controlled functions of image selection, calibration, digitization, damage mode identification, damage area and location measurement, damage pattern display, and data output. The GUIs developed for this aim will prove to be an invaluable tool in the completion of future research projects.

While the GUIs that were developed are able to complete analysis of the imported digital images, it is not optimized. The developer of the GUIs did not specialize in computer/software engineering and believes that much can be done to reduce the amount of CPU Usage that occurs while the program is running. The program was designed with the purpose of analyzing a particular subset of retrieved tibial inserts. If the program is to

be used to analyze inserts outside of the scope of the original grouping, additional work will need to be completed.

The third aim of this research assessed the differences in variations in damage modes and damage distribution between highly cross-linked and conventional polyethylene and posterior stabilized and PCL retaining TKR designs. Overall, a reduction in average medial and lateral damage areas was found in highly cross-linked polyethylene compared to conventional polyethylene. Also, there was a significant difference in lateral damage centroid locations between the two articular constraints.

The highly cross-linked polyethylene tibial inserts show a significant reduction in average medial and lateral damage areas compared to conventional polyethylene tibial inserts. Burnishing and striation impacted a greater number of highly cross-linked inserts than conventional ones in both comparison groups while pitting occurred at a lower frequency. This is significant in that it shows that the highly cross-linked polyethylene is achieving its design purpose – reduction in polyethylene debris particle generation and damage. There was a lower incidence of damage related to fatigue failure in highly cross-linked polyethylene than in conventional. In the instances where the frequency of damage occurred more readily in highly cross-linked inserts, it typically occurred at a lower percent area affected. The lateral damage centroid location was statistically significantly different between the two types of polyethylene, with highly cross-linked inserts experiencing damage more posteriorly. This could lose statistical significance with increased sample size or *in vivo* time and warrants further exploration.

Posterior stabilized TKR designs have more centrally located lateral damage

centroid locations and the PCL retaining designs have more centrally located medial damage centroid locations. In the Genesis II highly cross-linked articular designs the lateral damage centroids were statistically significantly different, with the posterior stabilized design centroid being located anteriorly and the PCL retaining design located posteriorly. With increasing sample size, although the statistical significance was lost, both articular constraint designs had the medial damage centroid located anteriorly to the lateral damage centroid. Although not much work has been done evaluating damage centroid location, the results of this work reflect the purpose with which the designs were made and are located in regions consistent with other published studies. The posterior stabilized design was created to constrain the amount of AP movement experienced by the TKR, as the post needed to replace the PCL whose purpose is to control AP translation in the natural joint. The damage centroid being located more centrally in the posterior retaining inserts than in the PCL retaining inserts shows the success of the design in controlling movement and is supported by the knowledge that posterior stabilized TKR designs have relatively symmetrical posterior femoral translation during flexion.[80] Out of the three constraint comparison groups, only Compare CONSTRAINT 3 had a statistically significant difference in the amount of wear experienced by the lateral bearing surface of the polyethylene inserts. As CONSTRAINT 3 was composed of devices of the same model and manufacturer, this could be attributed to that particular design and does not extrapolate across all models and manufacturers.

All inserts used in this work had relatively short *in vivo* lifespans. Intermediate results are important to assess, but long term outcomes hold more significance and merit.

Additional long-term inserts for both articular constraint and polyethylene type are necessary to strengthen the results found in Aim 3. Greater *in vivo* time could significantly impact the damage frequency and affected area percentages. Another way in which the significance of this work could be improved would be to increase the sample size. The standard deviations were high, raising the question of their validity. A larger sample size would help to clarify if the results from this work are more universally applicable by potentially reducing the standard deviations. It is interesting to note that statistical significance related to damage centroid location was achieved when only one brand of TKR designs were evaluated. Additional TKR models should be evaluated to determine if there is a difference in damage distribution for their design.

References:

1. Grupp TM, Kaddick C, Schwiesau J, Maas A, Stulberg SD. Fixed and mobile bearing total knee arthroplasty--influence on wear generation, corresponding wear areas, knee kinematics and particle composition. *Clin Biomech (Bristol, Avon)*. 2009;24(2):210-217. doi: 10.1016/j.clinbiomech.2008.11.006; 10.1016/j.clinbiomech.2008.11.006.

2. Furnes, O, B Espehaug, SA Lie, LB Engesaeter, SE Vollset, G Hallan, AM Fenstad, and L Havelin. Prospective studies of hip and knee prostheses - the norwegian arthroplasty register 1987 – 2004. *Procs 72nd AAOS Washington*. 2005.

3. Pradahan, NR, A Gambhir, and ML Porter. Survivorship analysis of 3234 primary knee arthroplasties implanted over a 26-year period. *The Knee*. 2006;13(1):7 - 11.

4. Kurtz S, Ong K, Lau E, Mowat F, Halpern M. Projections of primary and revision hip and knee arthroplasty in the united states from 2005 to 2030. *J Bone Joint Surg Am*. 2007;89(4):780-785. doi: 10.2106/JBJS.F.00222.

5. Rothwell AG, Hooper GJ, Hobbs A, Frampton CM. An analysis of the oxford hip and knee scores and their relationship to early joint revision in the new zealand joint registry. *J Bone Joint Surg Br*. 2010;92(3):413-418. doi: 10.1302/0301-620X.92B3.22913; 10.1302/0301-620X.92B3.22913.

6. Pynsent PB, Adams DJ, Disney SP. The oxford hip and knee outcome questionnaires for arthroplasty. *J Bone Joint Surg Br*. 2005;87(2):241-248.

7. Insall JN, Dorr LD, Scott RD, Scott WN. Rationale of the knee society clinical rating system. *Clin Orthop Relat Res*. 1989;(248)(248):13-14.

8. Naudie DD, Ammeen DJ, Engh GA, Rorabeck CH. Wear and osteolysis around total knee arthroplasty. *J Am Acad Orthop Surg*. 2007;15(1):53-64.

9. Scott RD. The evolving incidence and reasons for re-operation after fixed-bearing PCL retaining total knee arthroplasty. *J Bone Joint Surg Br*. 2012;94(11 Suppl A):134-136. doi: 10.1302/0301-620X.94B11.30830; 10.1302/0301-620X.94B11.30830.

10. Huang CH, Ho FY, Ma HM, et al. Particle size and morphology of UHMWPE wear debris in failed total knee arthroplasties--a comparison between mobile bearing and fixed bearing knees. *J Orthop Res*. 2002;20(5):1038-1041. doi: 10.1016/S0736-0266(02)00015-3.

11. Anderson, James, A Rodriguez, and D Chang. Foreign body reaction to biomaterials. *Semin Immunol*. 2008;20(2):86 - 100.

12. Wasielewski RC, Parks N, Williams I, Surprenant H, Collier JP, Engh G. Tibial insert undersurface as a contributing source of polyethylene wear debris. *Clin Orthop Relat Res*. 1997;(345)(345):53-59.

13. Gross TP, Lennox DW. Osteolytic cyst-like area associated with polyethylene and metallic debris after total knee replacement with an uncemented vitallium prosthesis. A case report. *J Bone Joint Surg Am*. 1992;74(7):1096-1101.

14. Heim CS, Postak PD, Greenwald AS. Factors influencing the longevity of UHMWPE tibial components. *Instr Course Lect*. 1996;45:303-312.

15. Harman M, Cristofolini L, Erani P, Stea S, Viceconti M. A pictographic atlas for classifying damage modes on polyethylene bearings. *J Mater Sci Mater Med*. 2011;22(5):1137-1146. doi: 10.1007/s10856-011-4303-x; 10.1007/s10856-011-4303-x.

16. Christen B, Neukamp M, Aghayev E. No difference in anterior tibial translation with and without posterior cruciate ligament in less invasive total knee replacement. *Knee Surg Sports Traumatol Arthrosc*. 2012;20(3):503-509. doi: 10.1007/s00167-011-1560-7; 10.1007/s00167-011-1560-7.

17. Blaha JD. The rationale for a total knee implant that confers anteroposterior stability throughout range of motion. *J Arthroplasty*. 2004;19(4 Suppl 1):22-26.

18. Suggs JF, Hanson GR, Park SE, Moynihan AL, Li G. Patient function after a posterior stabilizing total knee arthroplasty: Cam-post engagement and knee kinematics. *Knee Surg Sports Traumatol Arthrosc*. 2008;16(3):290-296. doi: 10.1007/s00167-007-0467-9; 10.1007/s00167-007-0467-9.

19. Kim YH, Sohn KS, Kim JS. Range of motion of standard and high-flexion posterior stabilized total knee prostheses. A prospective, randomized study. *J Bone Joint Surg Am*. 2005;87(7):1470-1475. doi: 10.2106/JBJS.D.02707.

20. Guo L, Yang L, Briard JL, Duan XJ, Wang FY. Long-term survival analysis of posterior cruciate-retaining total knee arthroplasty. *Knee Surg Sports Traumatol Arthrosc*. 2012;20(9):1760-1765. doi: 10.1007/s00167-011-1758-8; 10.1007/s00167-011-1758-8.

21. Lachiewicz PF, Soileau ES. Fifteen-year survival and osteolysis associated with a modular posterior stabilized knee replacement. A concise follow-up of a previous report. *J Bone Joint Surg Am*. 2009;91(6):1419-1423. doi: 10.2106/JBJS.H.01351; 10.2106/JBJS.H.01351.

22. Utzschneider S, Paulus A, Datz JC, et al. Influence of design and bearing material on polyethylene wear particle generation in total knee replacement. *Acta Biomater*. 2009;5(7):2495-2502. doi: 10.1016/j.actbio.2009.03.016; 10.1016/j.actbio.2009.03.016.

23. Markel D. Mechanical properties and faitgue performance of crosslinked polyethylene in total knee applications. *Seminars in arthroplasty*. 2003;14(4):222.

24. Benevenia J, Lee FY, Buechel F, Parsons JR. Pathologic supracondylar fracture due to osteolytic pseudotumor of knee following cementless total knee replacement. *J Biomed Mater Res*. 1998;43(4):473-477.

25. Engh GA, Dwyer KA, Hanes CK. Polyethylene wear of metal-backed tibial components in total and unicompartmental knee prostheses. *Society of Bone and Joint Surgery*. 1992;74-B:9-17.

26. Engh GA, Parks NL, Ammeen DJ. Tibial osteolysis in cementless total knee arthroplasty. A review of 25 cases treated with and without tibial component revision. *Clin Orthop Relat Res*. 1994;(309)(309):33-43.

27. Kane KR, DeHeer DH, Beebe JD, Bereza R. An osteolytic lesion associated with polyethylene wear debris adjacent to a stable total knee prosthesis. *Orthop Rev*. 1994;23(4):332-337.

28. Lewis PL, Rorabeck CH, Bourne RB. Screw osteolysis after cementless total knee replacement. *Clin Orthop Relat Res*. 1995;(321)(321):173-177.

29. Peters PC,Jr, Engh GA, Dwyer KA, Vinh TN. Osteolysis after total knee arthroplasty without cement. *J Bone Joint Surg Am*. 1992;74(6):864-876.

30. Rodriguez RJ, Barrack RL. Failed cementless total knee arthroplasty presenting as osteolysis of the fibular head. *J Arthroplasty*. 2001;16(2):239-242. doi: 10.1054/arth.2001.20543.

31. Sanchis-Alfonso V, Alcacer-Garcia J. Extensive osteolytic cystlike area associated with polyethylene wear debris adjacent to an aseptic, stable, uncemented unicompartmental knee prosthesis: Case report. *Knee Surg Sports Traumatol Arthrosc*. 2001;9(3):173-177.

32. Vernon BA, Bollinger AJ, Garvin KL, McGarry SV. Osteolytic lesion of the tibial diaphysis after cementless TKA. *Orthopedics*. 2011;34(3):224-20110124-30. doi: 10.3928/01477447-20110124-30; 10.3928/01477447-20110124-30.

33. Chang J, Yoo J, Hur M, Lee S, Chung Y, Lee C. Revision total hip arthroplasty for pelvic osteolysis with well-fixed cementless cup. *The Journal of Arthroplasty*. 2007;22(7):987.

34. Saleh KJ, Rand JA, McQueen DA. Current status of revision total knee arthroplasty: How do we assess results? *J Bone Joint Surg Am*. 2003;85-A Suppl 1:S18-20.

35. Koh KH, Moon Y, Lim S, Il Lee H, Shim JW, Park Y. Complete acetabular cup revision versus isolated liner exchange for polyethylene wear and osteolysis without loosening in cementless total hip arthroplasty. *Arch Orthop Trauma Surg*. 2011;131(11). doi: 10.1007/s00402-011-1338-x.

36. Restrepo C, Ghanem E, Houssock C, Austin M, Parvizi J, Hozack WJ. Isolated polyethylene exchange versus acetabular revision for polyethylene wear. *Clin Orthop Relat Res*. 2009;467(1):194-198. doi: 10.1007/s11999-008-0533-8.

37. Babis GC, Trousdale RT, Morrey BF. The effectiveness of isolated tibial insert exchange in revision total knee arthroplasty. *J Bone Joint Surg Am*. 2002;84-A(1):64-68.

38. Griffin WL, Scott RD, Dalury DF, Mahoney OM, Chiavetta JB, Odum SM. Modular insert exchange in knee arthroplasty for treatment of wear and osteolysis. *Clin Orthop Relat Res*. 2007;464:132-137.

39. Callaghan JJ, Reynolds ER, Ting NT, Goetz DD, Clohisy JC, Maloney WJ. Liner exchange and bone grafting: Rare option to treat wear & lysis of stable TKAs. *Clin Orthop Relat Res*. 2011;469(1):154-159. doi: 10.1007/s11999-010-1521-3.

40. Bloebaum RD, Rubman MH, Hofmann AA. Bone ingrowth into porous-coated tibial components implanted with autograft bone chips. analysis of ten consecutively retrieved implants. *J Arthroplasty*. 1992;7(4):483-493.

41. Bloebaum RD, Koller KE, Willie BM, Hofmann AA. Does using autograft bone chips achieve consistent bone ingrowth in primary TKA? *Clin Orthop Relat Res*. 2012;470(7):1869-1878. doi: 10.1007/s11999-011-2214-2.

42. Whiteside LA, Katerberg B. Revision of the polyethylene component for wear in TKA. *Clin Orthop Relat Res*. 2006;452:193-199. doi: 10.1097/01.blo.0000238802.90090.82.

43. Engh GA, Koralewicz LM, Pereles TR. Clinical results of modular polyethylene insert exchange with retention of total knee arthroplasty components. *J Bone Joint Surg Am*. 2000;82(4):516-523.

44. Mow CS, Wiedel JD. Structural allografting in revision total knee arthroplasty. *J Arthroplasty*. 1996;11(3):235-241.

45. Stockley I, McAuley JP, Gross AE. Allograft reconstruction in total knee arthroplasty. *J Bone Joint Surg Br*. 1992;74(3):393-397.

46. Hockman DE, Ammeen D, Engh GA. Augments and allografts in revision total knee arthroplasty: Usage and outcome using one modular revision prosthesis. *J Arthroplasty*. 2005;20(1):35-41. doi: 10.1016/j.arth.2004.09.059.

47. Haas SB, Insall JN, Montgomery W,3rd, Windsor RE. Revision total knee arthroplasty with use of modular components with stems inserted without cement. *J Bone Joint Surg Am*. 1995;77(11):1700-1707.

48. Peters CL, Hennessey R, Barden RM, Galante JO, Rosenberg AG. Revision total knee arthroplasty with a cemented posterior-stabilized or constrained condylar prosthesis: A minimum 3-year and average 5-year follow-up study. *J Arthroplasty*. 1997;12(8):896-903.

49. Drosos GI, Kazakos KI, Kouzoumpasis P, Verettas DA. Safety and efficacy of commercially available demineralised bone matrix preparations: A critical review of clinical studies. *Injury*. 2007;38 Suppl 4:S13-21.

50. Gruskin E, Doll BA, Futrell FW, Schmitz JP, Hollinger JO. Demineralized bone matrix in bone repair: History and use. *Adv Drug Deliv Rev*. 2012;64(12):1063-1077. doi: 10.1016/j.addr.2012.06.008; 10.1016/j.addr.2012.06.008.

51. Engh CA,Jr, Sychterz CJ, Young AM, Pollock DC, Toomey SD, Engh CA S. Interobserver and intraobserver variability in radiographic assessment of osteolysis. *J Arthroplasty*. 2002;17(6):752-759.

52. Dexel J, Kirschner S, Harman MK, Lutzner J. A rare case of bilateral large osteolysis following cemented and cementless total knee arthroplasties. *Acta Orthop*. 2012. doi: 10.3109/17453674.2013.752693.

53. Solomon LB, Stamenkov RB, MacDonald AJ, et al. Imaging periprosthetic osteolysis around total knee arthroplasties using a human cadaver model. *J Arthroplasty*. 2012;27(6):1069-1074. doi: 10.1016/j.arth.2011.09.012; 10.1016/j.arth.2011.09.012.

54. Crowninshield RD, Wimmer MA, Jacobs JJ, Rosenberg AG. Clinical performance of contemporary tibial polyethylene components. *J Arthroplasty*. 2006;21(5):754-761. doi: 10.1016/j.arth.2005.10.012.

55. Lu, YC, CH Huang, TK Chang, FY Ho, CK Cheng, and CH Huang. Wear-pattern analysis in retrieved tibial inserts of mobile-bearing and fixed-bearing total knee prostheses. *Journal of Bone and Joint Surgery*. 2010;92-B(4):500 - 507.

56. Hood RW, Wright TM, Burstein AH. Retrieval analysis of total knee prostheses: A method and its application to 48 total condylar prostheses. *J Biomed Mater Res*. 1983;17(5):829-842. doi: 10.1002/jbm.820170510.

57. Wright TM, Rimnac CM, Faris PM, Bansal M. Analysis of surface damage in retrieved carbon fiber-reinforced and plain polyethylene tibial components from posterior stabilized total knee replacements. *J Bone Joint Surg Am*. 1988;70(9):1312-1319.

58. Harman MK, Markovich GD, Banks SA, Hodge WA. Wear patterns on tibial plateaus from varus and valgus osteoarthritic knees. *Clin Orthop Relat Res*. 1998;(352)(352):149-158.

59. Harman MK, Banks SA, Hodge WA. Polyethylene damage and knee kinematics after total knee arthroplasty. *Clin Orthop Relat Res*. 2001;(392)(392):383-393.

60. Harman MK, Schmitt S, Rossing S, et al. Polyethylene damage and deformation on fixed-bearing, non-conforming unicondylar knee replacements corresponding to progressive changes in alignment and fixation. *Clin Biomech (Bristol, Avon)*. 2010;25(6):570-575. doi: 10.1016/j.clinbiomech.2010.03.013; 10.1016/j.clinbiomech.2010.03.013.

61. Harman MK, DesJardins J, Benson L, Banks SA, LaBerge M, Hodge WA. Comparison of polyethylene tibial insert damage from in vivo function and in vitro wear simulation. *J Orthop Res*. 2009;27(4):540-548. doi: 10.1002/jor.20743; 10.1002/jor.20743.

62. Harman MK, Banks SA, Hodge WA. Backside damage corresponding to articular damage in retrieved tibial polyethylene inserts. *Clin Orthop Relat Res*. 2007;458:137-144. doi: 10.1097/BLO.0b013e3180320b01.

63. Shi X, Shen B, Yang J, Kang P, Zhou Z, Pei F. In vivo kinematics comparison of fixed- and mobile-bearing total knee arthroplasty during deep knee bending motion. *Knee Surg Sports Traumatol Arthrosc*. 2012. doi: 10.1007/s00167-012-2333-7.

64. Namba RS, Inacio MC, Paxton EW, et al. Risk of revision for fixed versus mobile-bearing primary total knee replacements. *J Bone Joint Surg Am*. 2012;94(21):1929-1935. doi: 10.2106/JBJS.K.01363; 10.2106/JBJS.K.01363.

65. Pijls BG, Valstar ER, Kaptein BL, Nelissen RG. Differences in long-term fixation between mobile-bearing and fixed-bearing knee prostheses at ten to 12 years' follow-up: A single-blinded randomised controlled radiostereometric trial. *J Bone Joint Surg Br*. 2012;94(10):1366-1371. doi: 10.1302/0301-620X.94B10.28858.

66. Gee AO, Lee GC. Alternative bearings in total knee arthroplasty. *Am J Orthop (Belle Mead NJ)*. 2012;41(6):280-283.

67. O'Rourke MR, Callaghan JJ, Goetz DD, Sullivan PM, Johnston RC. Osteolysis associated with a cemented modular posterior-cruciate-substituting total knee design : Five to eight-year follow-up. *J Bone Joint Surg Am*. 2002;84-A(8):1362-1371.

68. Scuderi GR, Clarke HD. Cemented posterior stabilized total knee arthroplasty. *J Arthroplasty*. 2004;19(4 Suppl 1):17-21.

69. Ehrhardt J, Gadinsky N, Lyman S, Markowicz D, Westrich G. Average 7-year survivorship and clinical results of a newer primary posterior stabilized total knee arthroplasty. *HSS J*. 2011;7(2):120-124. doi: 10.1007/s11420-011-9196-1; 10.1007/s11420-011-9196-1.

70. Ginsel BL, Banks S, Verdonschot N, Hodge WA. Improving maximum flexion with a posterior cruciate retaining total knee arthroplasty: A fluoroscopic study. *Acta Orthop Belg*. 2009;75(6):801-807.

71. Seah RB, Pang HN, Lo NN, et al. Evaluation of the relationship between anteroposterior translation of a posterior cruciate ligament-retaining total knee replacement and functional outcome. *J Bone Joint Surg Br*. 2012;94(10):1362-1365. doi: 10.1302/0301-620X.94B10.28774.

72. Schuster AJ, von Roll AL, Pfluger D, Wyss T. Anteroposterior stability after posterior cruciate-retaining total knee arthroplasty. *Knee Surg Sports Traumatol Arthrosc*. 2011;19(7):1113-1120. doi: 10.1007/s00167-010-1364-1; 10.1007/s00167-010-1364-1.

73. Abdel MP, Morrey ME, Jensen MR, Morrey BF. Increased long-term survival of posterior cruciate-retaining versus posterior cruciate-stabilizing total knee replacements. *J Bone Joint Surg Am*. 2011;93(22):2072-2078. doi: 10.2106/JBJS.J.01143; 10.2106/JBJS.J.01143.

74. Li N, Tan Y, Deng Y, Chen L. Posterior cruciate-retaining versus posterior stabilized total knee arthroplasty: A meta-analysis of randomized controlled trials. *Knee Surg Sports Traumatol Arthrosc*. 2012. doi: 10.1007/s00167-012-2275-0.

75. Kurtz SM, Muratoglu OK, Evans M, Edidin AA. Advances in the processing, sterilization, and crosslinking of ultra-high molecular weight polyethylene for total joint arthroplasty. *Biomaterials*. 1999;20(18):1659-1688.

76. Premnath V, Harris WH, Jasty M, Merrill EW. Gamma sterilization of UHMWPE articular implants: An analysis of the oxidation problem. ultra high molecular weight poly ethylene. *Biomaterials*. 1996;17(18):1741-1753.

77. Muratoglu OK, Mark A, Vittetoe DA, Harris WH, Rubash HE. Polyethylene damage in total knees and use of highly crosslinked polyethylene. *J Bone Joint Surg Am*. 2003;85-A Suppl 1:S7-S13.

78. Kurtz SM, Gawel HA, Patel JD. History and systematic review of wear and osteolysis outcomes for first-generation highly crosslinked polyethylene. *Clin Orthop Relat Res*. 2011;469(8):2262-2277. doi: 10.1007/s11999-011-1872-4; 10.1007/s11999-011-1872-4.

79. Macdonald DW, Higgs G, Parvizi J, et al. Oxidative properties and surface damage mechanisms of remelted highly crosslinked polyethylenes in total knee arthroplasty. *Int Orthop*. 2013;37(4):611-615. doi: 10.1007/s00264-013-1796-6; 10.1007/s00264-013-1796-6.

80. Banks SA, Hodge WA. Implant design affects knee arthroplasty kinematics during stair-stepping. *Clin Orthop Relat Res*. 2004;(426)(426):187-193.

81. Banks SA, Hodge WA. 2003 hap paul award paper of the international society for technology in arthroplasty. design and activity dependence of kinematics in fixed and mobile-bearing knee arthroplasties. *J Arthroplasty*. 2004;19(7):809-816.

82. Delport HP, Banks SA, De Schepper J, Bellemans J. A kinematic comparison of fixed- and mobile-bearing knee replacements. *J Bone Joint Surg Br*. 2006;88(8):1016-1021. doi: 10.1302/0301-620X.88B8.17529.

83. Banks S, Bellemans J, Nozaki H, Whiteside LA, Harman M, Hodge WA. Knee motions during maximum flexion in fixed and mobile-bearing arthroplasties. *Clin Orthop Relat Res*. 2003;(410)(410):131-138. doi: 10.1097/01.blo.0000063121.39522.19.

84. Kawanabe K, Clarke IC, Tamura J, et al. Effects of A-P translation and rotation on the wear of UHMWPE in a total knee joint simulator. *J Biomed Mater Res*. 2001;54(3):400-406.

85. Utzschneider S, Harrasser N, Schroeder C, Mazoochian F, Jansson V. Wear of contemporary total knee replacements--a knee simulator study of six current designs. *Clin Biomech (Bristol, Avon)*. 2009;24(7):583-588. doi: 10.1016/j.clinbiomech.2009.04.007; 10.1016/j.clinbiomech.2009.04.007.

86. Willie BM, Foot LJ, Prall MW, Bloebaum RD. Surface damage analysis of retrieved highly crosslinked polyethylene tibial components after short-term implantation. *J Biomed Mater Res B Appl Biomater*. 2008;85(1):114-124. doi: 10.1002/jbm.b.30923.

87. Muratoglu OK, Ruberti J, Melotti S, Spiegelberg SH, Greenbaum ES, Harris WH. Optical analysis of surface changes on early retrievals of highly cross-linked and conventional polyethylene tibial inserts. *J Arthroplasty*. 2003;18(7 Suppl 1):42-47.

88. Muratoglu OK, Bragdon CR, Jasty M, O'Connor DO, Von Knoch RS, Harris WH. Knee-simulator testing of conventional and cross-linked polyethylene tibial inserts. *J Arthroplasty*. 2004;19(7):887-897.

89. Asano, Taiyo, M Akagi, IC Clarke, S Masuda, T Ishii, and T Nakamura. Dose effects of cross-linking polyethylene for total knee arthroplasty on wear performance and mechanical properties. *Journal of biomedical materials research.Part B, Applied biomaterials*. 2007;83-B(2):615 - 622.

90. Wang A, Yau SS, Essner A, Herrera L, Manley M, Dumbleton J. A highly crosslinked UHMWPE for CR and PS total knee arthroplasties. *J Arthroplasty*. 2008;23(4):559-566. doi: 10.1016/j.arth.2007.05.007; 10.1016/j.arth.2007.05.007.

91. Blunn GW, Joshi AB, Minns RJ, et al. Wear in retrieved condylar knee arthroplasties. A comparison of wear in different designs of 280 retrieved condylar knee prostheses. *J Arthroplasty*. 1997;12(3):281-290.